



Technical papers

---

## Rocketry aerodynamics

Aspirepace technical papers

Author: Rick Newlands





## Table of Contents

Introduction.....	4
Nomenclature.....	4
1: Data sources.....	5
2: The flight of finned rocket vehicles.....	6
Yawing motion.....	6
Fin Stabilisation.....	6
Space axes.....	6
3: Aerodynamic forces.....	7
Pressure distribution.....	7
Forces and force coefficients.....	7
Axes systems.....	8
Lift (Normal force).....	9
The Barrowman analysis.....	10
Extending the Barrowman results.....	12
Forebody lift at near-zero angle of attack.....	13
Forebody centre of pressure at near-zero angle of attack.....	13
Forebody lift at finite angle of attack.....	14
Forebody centre of pressure at finite angle of attack.....	16
Boat-tailing: lift.....	18
Boat-tailing: centre of pressure.....	18
Fin lift at zero angle of attack.....	19
Fin lift at finite angle of attack.....	20
Three fins.....	21
Fins centre of pressure.....	21
Interference effects on lift.....	22
Interference effects on centre of pressure.....	26
4: Stability.....	29
Barrowman:.....	29
Static stability.....	29
Aeroplane static stability.....	31
Barrowman versus ESDU static stability.....	31
One calibre.....	32
Dynamic stability.....	32
Dynamic effects.....	32



Aerodynamic damping .....	33
Cross-spin force and damping moment .....	35
Evaluation .....	35
5: The effect of viscosity.....	37
The boundary Layer .....	37
Viscous corrections .....	39
Boattail.....	41
Viscous effect on static stability .....	41
6: Drag .....	43
The missing drag conundrum.....	43
Overall estimate .....	43
Boat-tailing .....	45
Valid drag assumptions.....	45
Subsonic drag: Mach number $< 0.8$ .....	46
Skin friction drag .....	46
Profile drag.....	46
Base drag.....	46
Excrescence drag .....	47
The Transonic zone: $0.8 < \text{Mach number} < 1.2$ (ish) .....	47
Base drag.....	47
Excrescence drag .....	47
Supersonic drag: $1.2 > \text{Mach number} > 5$ ish .....	47
Skin friction .....	47
Wave (profile) drag.....	47
Base drag.....	47
Excrescence drag .....	48
7: Measuring the aerodynamic coefficients .....	49
Aerodynamic damping.....	49
Measurement of $CM_{CG}$ : the ‘wavelength of yaw’ .....	49
8: Applicability and accuracy .....	51
Glossary .....	53
References.....	56



## Introduction

Aerodynamics is one of the fundamental forces affecting the flight of our rocket vehicles. For example, if you switch the atmosphere off in your trajectory simulations (set drag equal to zero) you will find that your vehicles will reach an apogee around nine times higher! We really are at the bottom of a deep sea of thick air.

Unfortunately, it can be difficult to get good aerodynamic data, and even when you do the data isn't terribly exact (expect it to be plus or minus 15% or so at best). With this uncertainty in mind, the following is a guide to the aerodynamics of our vehicles, assuming they have fixed fins for stability.

I'd strongly advise programming the equations in this paper, perhaps into a spreadsheet.

Words in **bold** are listed in the glossary at the end of the paper.

## Nomenclature

$\alpha$  = Angle of attack (radians or degrees)  
 $\beta$  = subsonic or supersonic similarity parameter  
 $\delta^*$  = (displacement) thickness of the boundary layer (m)  
 $\theta$  = Pitch angle (radians)  
 $\dot{\theta}$  = Pitch rate (radians/second). The dot is Newton's notation for time rate of change.  
 $\phi$  = Climb angle (also known as flight path angle or trajectory angle), (radians)  
 $\rho$  = Atmospheric density (kg/m<sup>3</sup>)  
 $A$  = Acceleration (m/sec<sup>2</sup>)  
 $C_A$  = axial force coefficient (dimensionless)  
 $C_C$  = centroid of planform area coefficient ( $2X_p / L$ )  
 $C_D$  = Drag coefficient (dimensionless)  
 $C_F$  = mean skin-friction coefficient (dimensionless)  
 $C_H$  = damping moment (dimensionless)  
 $C_L$  = Lift coefficient (dimensionless)  
 $C_M$  = (pitching) moment coefficient (dimensionless)  
 $C_{M\alpha}$  = gradient of the pitching moment coefficient curve  
 $C_N$  = Normal force coefficient (dimensionless)  
 $C_{N\alpha}$  = Gradient of Normal force coefficient per radian angle of attack (1/radian)  
 $C_{NC}$  = lift contribution from the 'cross flow' around the circumference  
 $C_P$  = planform area coefficient ( $S_p/dL$ ), or alternatively, = pressure coefficient  
 $C_R$  = root chord length (m)  
 $C_T$  = tip chord length (m)  
 $d$  = Diameter of (thickest part of) the fuselage (m)  
 $d_R$  = boat-tail smaller diameter (m)  
 $I$  = moment of inertia (kgm<sup>2</sup>)  
 $L$  = overall length of the vehicle (m)  
 $L_C$  = length of cylindrical portion of forebody (m)  
 $L_F$  = length of fin midchord (m)  
 $L_N$  = length of the nosecone (m)  
 $L_T$  = boat-tail length (m)  
 $m$  = mass (kg)  
 $M$  = moment (Nm)  
 $N$  = normal force (N)  
 $n$  = number of fins (3 or 4)  
 $q$  = dynamic pressure (Nm<sup>2</sup>)  
 $r$  = fuselage radius (m)  
 $S$  = Cross-sectional area of (thickest part of) the fuselage (m<sup>2</sup>)  
 $s$  = fin semi-span (root chord to tip chord) or net semi span (m)  
 $S_p$  = planform area (m<sup>2</sup>)  
 $V$  = Velocity (m/sec)



## Technical papers

---

$X$  = centre of pressure position (m)

$X_p$  = centroid of planform area (m)

### **1: Data sources**

In the USA, they have access to Datcom data to give aerodynamic data for rocket vehicles.

Here in the U.K. we tend to use ESDU sheets (Engineering Sciences Data Units): Many years ago, the Royal Aeronautical Society tasked its members with gathering all sorts of knowledge on aerodynamics and aircraft design, and presenting it as a series of free papers. Then ESDU got hold of these papers, re-collated them, and now charge for them.

Sadly, it isn't possible to buy individual ESDU sheets, instead ESDU charge an annual subscription, which I'm told is relatively inexpensive compared to other subscription-only electronic journals, but is still a lot of money.

Students of Universities that have subscribed to ESDU can download ESDU papers for free by obtaining an ATHENS password: get any students you know to download the papers you need!

Be warned though, ESDU papers are hard work, and they reference other ESDU papers; check how many you need.

## 2: The flight of finned rocket vehicles

### Yawing motion

Suppose that the rocket is rotating about an axis perpendicular to its longitudinal axis. That is to say, it is turning end over end, but very slowly.

In ballistic parlance, this type of rotation is called a “yawing” motion; Aerodynamicists used to working with aircraft would tend to refer to a yawing motion in the vertical plane as “pitching”, whereas a yawing motion in the horizontal plane is called either yawing or “sideslipping”.

### Fin Stabilisation

A common means of preventing, or at least of restraining, a yawing motion is by the use of fins at the rear end of the rocket. These fins play a role analogous to the feathers on an arrow. Should the rocket vehicle find itself moving crosswise through the air, the wind action on the fins at the rear tends to push them back into line and so restores the rocket to head-on flight.

The net result is that for fin-stabilized rockets a yawing/pitching motion is usually oscillatory in nature; in fact, the rocket rotates back and forth in some plane as though it were a pendulum performing damped harmonic oscillations.

### Space axes

A rocket can yaw in two different planes at once. Commonly the yawing motions in the two planes will be out of phase. The result is a sort of corkscrew motion of the rocket, known as “conical yaw.” Since this gyration is compounded of two simple harmonic yawing motions, one in each of two different planes, it will suffice to work out the equations of motion for yawing in a single plane.

In this plane we fix an axis of reference. We denote by  $\theta$  the angle between the reference axis and the longitudinal axis of the rocket; this is the *Pitch angle*.

$\phi$  is the angle between the reference axis and the direction of motion of the rocket: known as either the *Trajectory angle*, *Climb angle*, or *Flight Path angle*.

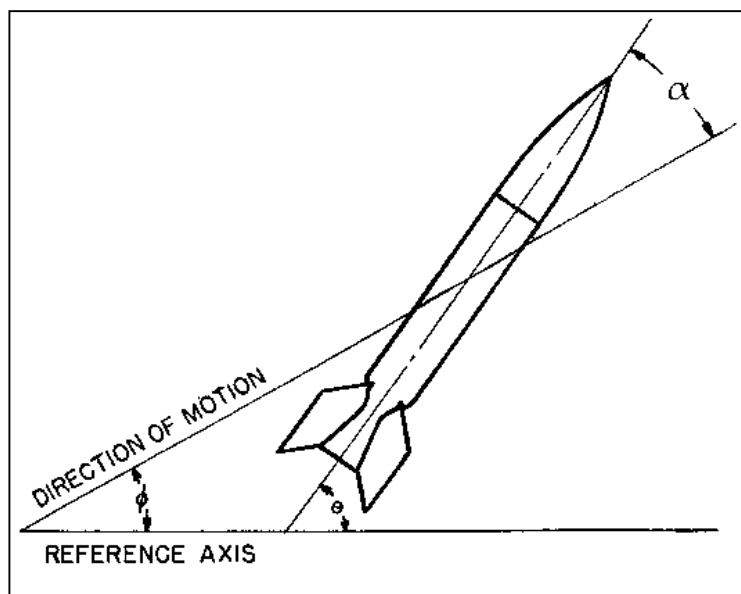
We denote by  $\alpha$  the angle between the longitudinal axis of the rocket and the direction of motion of the rocket, which is also the direction of the incoming air. Then  $\alpha$  is the angle of yaw, and we have:

$$\alpha = \theta - \phi \quad (\text{equ. 2.1})$$

Aerodynamicists used to working with aircraft would refer to a yaw angle in the vertical plane as the **angle of attack**  $\alpha$ , whereas in the horizontal plane it would be the *angle of sideslip*  $\beta$ .

These angles are illustrated in this sketch.

One designates the positive and negative directions for  $\phi$ ,  $\theta$  and  $\alpha$  in such a way that all three are positive for the configuration shown.

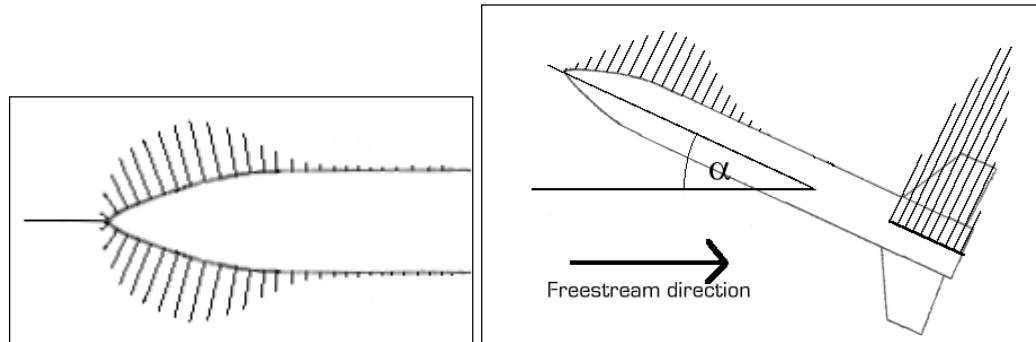


### 3: Aerodynamic forces

#### Pressure distribution

As the rocket vehicle moves through the air, the local airflow over and around it is forced to change velocity. The changes in velocity cause a complex pressure field distributed over the area of its 'skin', in accordance with **Bernoulli's principle**.

At low **subsonic** speeds, the air is essentially *incompressible*, that is, the density of the air doesn't change at all as the air changes speed around the vehicle. Above about Mach 0.7 however, *compressibility* effects (changing density) start to appear.



The picture on the left shows a representation of pressure around the nose at zero angle of attack. These lines represent suction, *except* for the very tip of the nose where there is a **stagnation point**. The flow is symmetrical about the fuselage long axis, so is called *axisymmetric flow*.

As the angle of attack is increased, the pressure distribution on the lower surfaces increases, while that on the upper reduces (a suction); the picture on the right is representative of the difference in the pressure distribution around the nose and fins at high angle of attack.

The lines show different axes that the pressure distribution can be transformed to: on the left is the raw pressure measured perpendicular to the skin whereas on the right the individual pressure readings have been resolved into an axis normal to the vehicle long axis. Not shown is the distribution transformed into an axis parallel with the vehicle long axis.

Note how the forces carry backward from the nose to the forward fuselage section. Both of these areas together are called the **forebody**.

As you can see, the main pressure regions occur at the forebody and the fins only.

#### Forces and force coefficients

The pressure distribution can then be integrated over the entire skin area to yield aerodynamic forces, which act at their centroid of the pressure distribution, or '**centres of pressure**'.

At the dawn of aerodynamics, the values of pressure in the pressure distribution, and hence the integrated aerodynamic forces, were found to be a product of:

$$F = q S C$$

where the constant '*C*' is known as an *aerodynamic coefficient* and *q* is **dynamic pressure**. So:

$$force = \frac{1}{2} \rho V^2 S C_f \quad (\text{equ. 3.1})$$

where  $S$  is some reference area and  $C_f$  is the aerodynamic force coefficient.

**N.B.** When using aerodynamic coefficients in the above formula, always state which reference area is being used:

For the integration of pressure distribution, the actual skin area 'S<sub>skin</sub>' is obviously used.

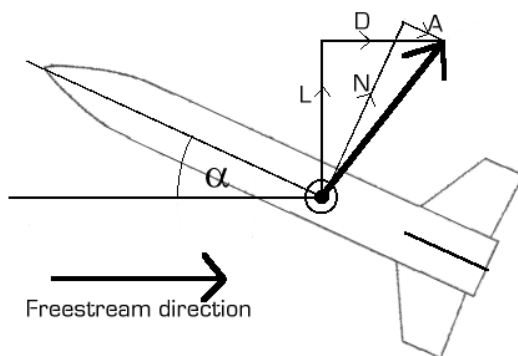
But for wing/fin calculations, the surface area of one side of the fin in plan view (as seen from above) is used, which is referred to as *planform area*.

Finally, the reference area in rocketry is taken as the cross-sectional area of the fattest part of the fuselage 'S<sub>cross</sub>' (see glossary).

When converting aerodynamic coefficients between these different reference areas, a conversion factor needs to be applied, such as the ratio of S<sub>fin</sub> over S<sub>cross</sub>.

### Axes systems

There are two popular aerodynamic force axes systems in use: *Wind axes* wherein the forces are referenced to the **freestream** flow direction (the incoming 'wind'), and *Body axes* wherein the axes are the geometric axes of the vehicle such as axes of symmetry.

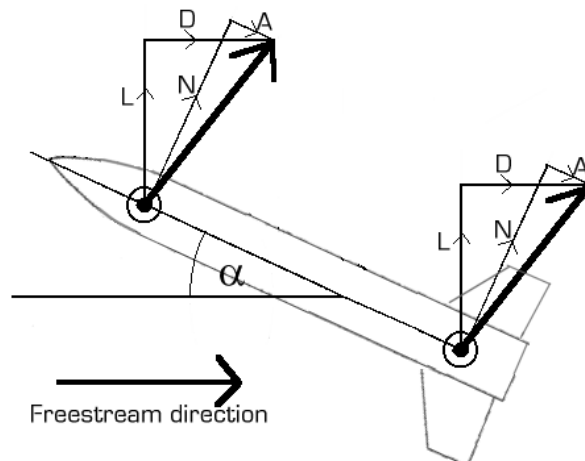


Traditionally, aircraft aerodynamicists use Wind axes, whereas rocketry aerodynamicists use Body axes.

The aerodynamic force components, when resolved into Wind axes, are known as *Lift (L)* and *Drag (D)*, whereas if resolved into Body axes are called *Normal force (N)* and *Axial force (A)*.

At the small angles of attack ( $\alpha$ ) experienced by our vehicles, the two axis systems are effectively coincidental, so either terminology will do. So when I refer to Lift, I'm really referring to Normal force.

Here the aerodynamic forces have been split into those from the nosecone (forebody) and those from the fins, acting at their respective centres of pressure. Splitting the forces like this is useful for stability analyses and structural calculations.





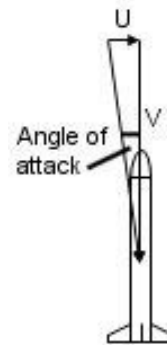
**Lift (Normal force)**

When the vehicle comes off the launcher and encounters the wind, or later on when it is hit by a gust or turbulence, the vehicle will pull an angle of attack.

Surprisingly large forces normal to the centreline of the airframe (lift forces) can be created by these gusts and other transient wind effects:

The sudden gust velocity vector 'U', when added to the vehicle's airspeed vector 'V', causes a small angle of attack  $\alpha$ :

$$\alpha = \tan^{-1} \left( \frac{U}{V} \right) \quad (\text{equ. 3.2})$$



It's this angle of attack that creates lift forces that create the side-loads on the fuselage. The deleterious effects of these lift forces on the structure is covered in our website paper 'Rocket vehicle loads and airframe design'.

The destabilising effects of the wind is covered later in the section on stability.

Surfaces that operate predominately at non-zero angles of attack are known as *Wings* whereas surfaces that operate predominately at zero angle of attack and have equal upper and lower surface curvature are known as *Fins*.

This is only a difference in terminology.

From the equation above, the lift force is defined as:  $Lift = \frac{1}{2} \rho V^2 S C_L$  (equ. 3.3)

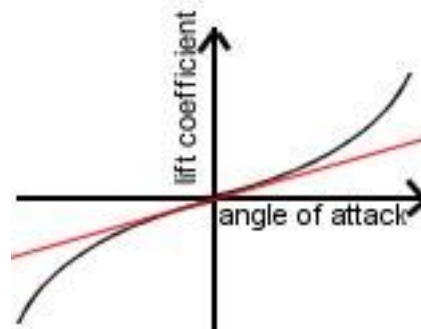
In rocketry, reference area S is taken as the cross-section of the thickest part of the fuselage, whereas in aircraft aerodynamics it is the wing area, so take care to use the correct reference area; convert from one to the other if necessary.

$C_L$  is the *Lift coefficient*. This is rather a misnomer, as 'coefficient' is supposed to apply to numbers that don't vary. Infact,  $C_L$  varies with angle of attack and **Mach number**.

The graph of lift coefficient versus angle of attack is known as the *Lift curve*. The gradient of this graph is known as the *Lift curve slope*.

When investigating the lift at very small angles of attack (tending to zero angle of attack) we tend to use the lift curve *slope* rather than the lift curve.

That's because for a symmetrical fin (same upper and lower surface shape) or a symmetrical forebody, the lift is zero at zero angle of attack and is therefore of no use for analysis.



The lift curve slope, on the other hand, is non-zero at zero angle of attack (tangent shown in red here) so is much more numerically useful:

The 'lift' (Normal force) curve slope at zero angle of attack is designated:  $C_{N\alpha 0}$

We tend to only require the lift coefficient at very small angles of attack, as rocketry angles of attack generally don't get very high. Infact for stability analyses (see later) we only need this lift curve slope at zero angle of attack.

This requirement for only small angles of attack is just as well: long, narrow, aircraft wings with high **aspect ratio** have a nice, simple linear relationship between lift coefficient and angle of attack:  $C_L = C_{L\alpha} \alpha$  (equ. 3.4)

where  $\alpha$  is angle of attack and  $C_{L\alpha}$  is the (constant) lift curve slope.

But the very low aspect ratio fins we're forced to use for rocketry, which also have a large angle of leading edge sweepback (see **Geometric definitions** in the glossary) have a very non-linear relationship with angle of attack.

And for the forebody lift it's even worse: a Royal Aeronautical Society equation for forebody Normal force coefficient (based on extensive windtunnel results) is:

$$C_N = C_{N\alpha 0} \sin \alpha \cos \alpha + B \sin^2 \alpha \quad (\text{equ. 3.5})$$

Where  $\sin^2 \alpha = (\sin \alpha)^2$  and  $C_{N\alpha 0}$  is as above.

We'll use this equation for forebody lift; for small angles of attack the  $\sin^2 \alpha$  term is very small and we'll ignore it.

For near-zero angles of attack the first term is equivalent to just  $\alpha$  using the small angle approximations  $\sin \alpha = \alpha$  and  $\cos \alpha = 1$  (in radians) (equ.s 3.6)

The lift of any boat-tail added is also highly non-linear.

### The Barrowman analysis

NASA aerodynamicist and rocketeer James Barrowman decided to try and calculate the lift coefficient (Normal coefficient), and centres of pressure, of the forebody and fins (and boat-tail) of a rocket vehicle (Ref 1) at near-zero angle of attack.

By mathematically modelling the flow around the vehicle he derived some fairly simple equations by neglecting the effects of **viscosity** and **freestream** Mach number, and yet as we'll see his equations give very accurate results compared to the more detailed equations we'll use later on.

He found that the lift of the fuselage at near-zero angle of attack was zero, and that the lift curve slope for the nose at zero angle of attack is 2.0 for all typical nosecone shapes:

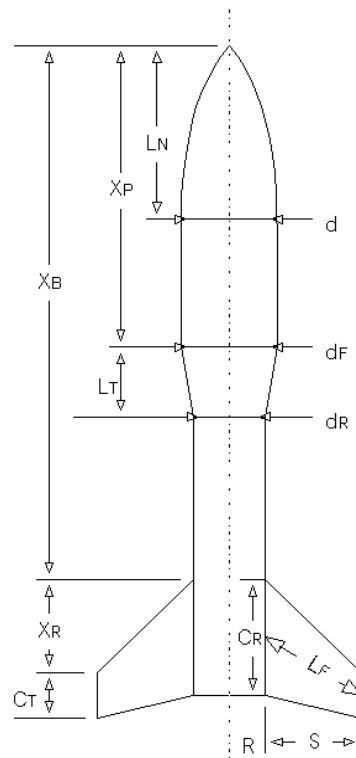
$$C_{N\alpha 0 nose} = 2.0 \quad (\text{per radian}) \quad (\text{equ. 3.7})$$

The fins lift curve slope at zero alpha he calculated in two parts; first, the lift of the fins alone:

$$C_{N\alpha 0 fin} = \frac{4n\left(\frac{s}{d}\right)^2}{1 + \sqrt{1 + \left(\frac{2L_F}{C_R + C_T}\right)^2}} \quad (\text{per radian}) \quad (\text{equ. 3.8})$$

And then using data from Ref. 3 he added the effect of the air flowing over the fuselage ahead of the fins:

$$\text{Interference factor} = 1 + \frac{r}{s+r} \quad (\text{equ. 3.9})$$





which you multiply the  $C_{N\alpha 0 fin}$  by.

In these equations:

- $n$  = number of fins (3 or 4)
- $d$  = fuselage diameter
- $r$  = fuselage radius
- $s$  = fin semi-span (NOT area)
- $L_F$  = length of midchord
- $C_R$  = root chord length
- $C_T$  = tip chord length

For the straight-cone boat-tail he realised that the lift of a boat-tail is negative, i.e. it's in the opposite direction to the fin and nose lift.

Its lift he derived as:

$$C_{N\alpha 0 boat} = -2 \left( 1 - \left( \frac{d_R}{d} \right)^2 \right) \text{ (per radian) (equ. 3.10)}$$

which is negative.  $d_R$  is the boat-tail smaller diameter.

The equation for calculating the centre of pressure  $X$  of any aerodynamic surface at zero angle of attack is:

$$\frac{X}{d} = - \frac{C_{m\alpha 0}}{C_{N\alpha 0}} \text{ (equ. 3.11)}$$

where  $C_{m\alpha 0}$  is the gradient of the **pitching moment coefficient** curve (per radian) at zero angle of attack measured about the nosetip. This gives the centre of pressure position measured aft of the nosetip. Note that this formula gives the centre of pressure position in **calibres**. Multiply by the fuselage diameter ' $d$ ' to get metres.

Using this formula, Barroman calculated the centre of pressure of a tangent-ogive nosecone (the shape most of our nosecones happen to be) as:

$$X_{nose} = 0.466 L_N \text{ (equ. 3.12)}$$

where  $L_N$  is the length of the nosecone (in metres), measuring from the nosetip aft. This gives  $X_{nose}$  in metres.

For the fins centre of pressure (metres aft of nosetip) he derived:

$$X_{Fins} = X_B + \frac{X_R}{3} \left( \frac{C_R + 2C_T}{C_R + C_T} \right) + \frac{1}{6} \left( C_R + C_T - \frac{C_R C_T}{C_R + C_T} \right) \text{ (equ. 3.13)}$$

Where  $X_R$  and  $X_B$  are lengths defined in the diagram on the previous page.

For the straight-cone boat-tail centre of pressure (metres aft of nosetip) he derived:

$$X_{boat} = X_P + \frac{L_T}{3} \left( 1 + \frac{1 - \frac{d}{d_R}}{1 - \left( \frac{d}{d_R} \right)^2} \right) \text{ (equ. 3.14)}$$



where  $X_P$  is a length defined in the diagram on the previous page, and  $L_T$  is the boat-tail length.  $d_R$  is the boat-tail smaller diameter.

### Extending the Barrowman results

Now Barrowman sensibly restricted his analysis to very low Mach numbers (technically zero Mach) so as not to have to add-in the effect of Mach number to his equations. This is reasonable for vehicles powered by solid-propellant motors because you only need to worry about their stability at launch (low airspeeds).

This is because their *centre of gravity* (CG) moves nosewards as propellant is used up from the tailwards motor, which makes them much more stable as burn-time passes.

For Hybrids however, their CG can even track tailwards with burn-time, so their stability needs to be monitored throughout the burn (at the very least, check their burnout stability as well).

Another limitation of the Barrowman analysis is that it is only valid for near-zero angles of attack: his basic assumption of constant aerodynamic coefficients breaks down above an angle of, say, 5 degrees or more; they then become functions of angle of attack.

Unfortunately, the main cause of vehicle instability and/or severe angular deviation of the trajectory is caused by the moderate angle of attack that can occur when a rocket vehicle leaves a launcher at too low an airspeed and meets the wind.

In particular, we'll see that the overall centre of pressure shifts nosewards with angle of attack, which reduces the stability.

I think I can say with some justification that if the use of Barrowman's small angle approximations becomes invalid here, then your launcher is too short for your vehicle; a rocket vehicle should leave its launcher with a high enough airspeed that the wind can't then cause a noticeable angle of attack. Almost every launcher I've ever seen in the **HPR** world is way too short! (Ours, cough, is 15 metres tall.)

Using ESDU data (Ref. 4), we can add the effects of Mach number, and we can also find the effect of angle of attack: we need to investigate the moderate angle of attack that the rocket vehicle pulls just after it leaves a short launcher (still at a low **subsonic** airspeed) and encounters the wind. (At higher airspeeds the angles of attack are very low as the airspeed vector is much larger than the wind vector, see equ. 3.2).

The ESDU sheets calculate the aerodynamics assuming the boat-tail isn't there, but with the overall length of the vehicle  $L$  the same as the length with boat-tail added, i.e. the boat-tail's just a cylinder.

They then add corrections for the boat-tail (keeping the overall vehicle length the same) i.e. they assume you've 'stuck the rear of the vehicle in a pencil sharpener' to sharpen it down to form a boat-tail.



Forebody lift at near-zero angle of attack

Firstly for the effect of freestream Mach number on the forebody alone (no boat-tailing), here is ESDU 89008  $C_{N\alpha 0nose}$  data (figure 1) for several length-to-diameter (calibre) ratios of tangent-ogive nosecones, assuming that the cylindrical portion of the fuselage is longer than 10 calibres:

Mach number	LN/d = 1.5 $C_{N\alpha 0nose}$ (per radian)	LN/d = 3 $C_{N\alpha 0nose}$ (per radian)	LN/d = 5 $C_{N\alpha 0nose}$ (per radian)	LN/d = 7 $C_{N\alpha 0nose}$ (per radian)
0	2	2	2	2
0.3	2.01	2.01	2.01	2.01
0.4	2.02	2.02	2.02	2.02
0.5	2.03	2.03	2.03	2.03
0.6	2.05	2.05	2.05	2.05
0.7	2.06	2.06	2.06	2.06
0.8	2.1	2.1	2.1	2.1
0.9	2.16	2.16	2.16	2.16
1	2.3	2.3	2.3	2.3
1.05	2.36	2.36	2.36	2.36
1.1	2.4	2.4	2.4	2.4
1.15	2.38	2.37	2.37	2.38
1.2	2.37	2.32	2.3	2.30
1.3	2.35	2.27	2.21	2.21
1.4	2.35	2.25	2.16	2.13
1.5	2.35	2.24	2.12	2.08
1.75	2.37	2.26	2.08	2.03
2	2.40	2.31	2.08	2.01
2.25	2.42	2.36	2.12	2.03
2.5	2.45	2.4	2.15	2.06
3	2.48	2.49	2.22	2.10
3.5	2.51	2.57	2.28	2.14
4	2.53	2.63	2.34	2.18
4.5	2.56	2.67	2.39	2.21
5	2.57	2.7	2.43	2.24

This data is for near-zero angle of attack. Note that for zero Mach we get the Barrowman result of 2.0, but at higher airspeeds the lift is greater, which is more de-stabilising: we'll need bigger fins.

Note that all the curves are identical up to Mach 1.1

For length-to-diameter ratios in between those given in this table, simply linearly interpolate the data.

ESDU 89009 also gives data for shorter fuselages, and for other nosecone types.

Forebody centre of pressure at near-zero angle of attack

From ESDU 89009 figure 5, here is the 'zero' angle of attack centre of pressure  $\frac{X_{nose\_alpha}}{d}$  i.e. in calibres, for tangent-ogive nosecones (no boat-tailing yet) at various freestream Mach numbers and for various LN/d ratios. Again for cylindrical fuselage lengths greater than 10 calibres.



Measure the position aft of the nosetip.

Mach number	$L_N/d = 1.5$	$L_N/d = 2$	$L_N/d = 3$	$L_N/d = 5$	$L_N/d = 5$	$L_N/d = 6$	$L_N/d = 7$
0	0.466 $L_N/d$	0.466 $L_N/d$	0.466 $L_N/d$	0.466 $L_N/d$	0.466 $L_N/d$	0.466 $L_N/d$	0.466 $L_N/d$
1.0	0.466 $L_N/d$	0.466 $L_N/d$	0.466 $L_N/d$	0.466 $L_N/d$	0.466 $L_N/d$	0.466 $L_N/d$	0.466 $L_N/d$
2.0	0.73	1.02	1.59	2.1	2.6	3.02	3.35
3.0	0.93	1.25	1.84	2.4	2.88	3.23	3.43
4.0	1.2	1.52	2.08	2.6	3.04	3.43	3.74
5.0	1.35	1.62	2.12	2.6	3.04	3.43	3.74

Note that the centre of pressure position is exactly the same as Barrowman's result for Mach numbers up to 1.0 (0.466 times  $L_N/d$ , i.e. in calibres)

#### Forebody lift at finite angle of attack

Now we want to investigate the lift of the forebody at low subsonic angles of attack, for which we need ESDU 89014 (which deals with angles of attack up to 90 degrees and speeds up to Mach 5).

The formula for calculating the Normal coefficient  $C_N$  is nearly identical to the old RAs society formula given earlier (equ. 1.3), and is:

$$C_N = C_{N\alpha 0} \sin \alpha \cos \alpha + \frac{4L}{\pi d} C_{NC} C_{PL} \quad (\text{equ. 3.14})$$

Where  $C_{N\alpha 0}$  is the lift curve slope at zero alpha we got earlier, and  $L$  is total vehicle length, again assuming no boat-tailing yet.

Because as we'll see shortly, these two terms have different centres of pressure, we'll split them up into:

$$C_{Nfore} = C_{N\alpha 0} \sin \alpha \cos \alpha \quad (\text{equ. 3.15})$$

$$C_{Ncrossflow} = \frac{4L}{\pi d} C_{NC} C_{PL} \quad (\text{equ. 3.16})$$

$C_{NC}$  is the contribution from the 'cross flow' or the airflow component flowing around the circumference of the fuselage at angle of attack. (We'll assume symmetric vortices are created by this cross flow, see ESDU 89014).

For our naturally-stable finned vehicles, they'll only pull a moderate angle of attack at low subsonic speeds; at higher speeds they'll only pull one or two degrees. So we only need to be able to calculate the cross flow properly for moderate angles of attack at low subsonic speeds:

$C_{NC}$  is obtained from figure 1a of ESDU 89014 for angles of attack up to 30 degrees, and we'll just concentrate on Mach numbers up to 0.5:

Angle of attack (degrees)	0	5	10	15	20	25	30
$C_{NC}$ for Mach < 0.5	0.000	0.005	0.015	0.035	0.065	0.110	0.175



For higher airspeeds (above Mach 0.5) we can use a different approach, as the angles of attack pulled as the vehicle encounters gusts decreases with forward airspeed; they'll only be one or two degrees (see equ. 3.2). So what we'll do is derive a  $C_{N\alpha 0\_crossflow}$  term, i.e. the lift-curve slope of cross flow with angle of attack at zero angle of attack. This will be adequate for small angles of attack, and it turns out that we'll need this term anyway later on for stability analyses.

What we'll do is measure the  $C_{NC}$  value at a small angle (5 degrees) from ESDU 89014 figure 1a, then divide this by 5 degrees to estimate the gradient  $\left(\frac{d(C_{NC})}{d\alpha}\right)$  of the  $C_{NC}$  versus angle of attack curve at near-zero angle of attack. Then we can convert this to a  $C_{N\alpha 0\_crossflow}$  term using equation 3.16:

$$C_{N\alpha 0\_crossflow} = \frac{4}{\pi} \frac{L}{d} C_{PL} \left(\frac{d(C_{NC})}{d\alpha}\right)_{at\ zero\ \alpha} \quad (\text{per radian}) \quad (\text{equ. 3.17})$$

$C_{NCrossflow}$  is then just equal to  $C_{N\alpha 0\_crossflow}$  times angle of attack (in radians).

So here's a table of  $\left(\frac{d(C_{NC})}{d\alpha}\right)_{at\ zero\ \alpha}$  versus Mach number,

which I got from ESDU 89014 figure 1a, remembering to convert the 5 degrees into radians in order to get  $C_{N\alpha 0\_crossflow}$  in radians<sup>-1</sup> like the other  $C_{N\alpha 0}$ 's.

Mach number	$\left(\frac{d(C_{NC})}{d\alpha}\right)_{at\ zero\ \alpha}$ (per radian)
0	0.063
0.5	0.068
0.7	0.069
0.8	0.069
0.9	0.067
1.0	0.066
1.2	0.063
1.5	0.057
2.0	0.060
2.5	0.066
3.0	0.077
3.5	0.092
> 4.0	0.115

In the above equations,  $C_{PL}$  is the *planform area coefficient* which is calculated in ESDU 77028 as:

$$C_{PL} = C_{Pf} \frac{L_N}{L} + \frac{L_m}{L} + C_{pa} \frac{L_T}{L} \quad (\text{equ. 3.18})$$

where  $L_N$ ,  $L_m$ , and  $L_T$ , are the lengths of the nosecone, parallel midsection, and boat-tail respectively.  $L$  is the total vehicle length.



In this equation  $C_{Pf}$  is the nosecone planform area coefficient and for a tangent ogive is equal to:

$$C_{Pf} = \frac{1}{2} \left( \frac{(F+1)^2}{\sqrt{2F+1}} \sin^{-1} \left( \frac{\sqrt{2F+1}}{F+1} \right) - F \right) \quad (\text{equ.3.19}) \text{ from ESDU 77028 appendix A4.3}$$

Where  $F = \frac{1}{2} \left( 4 \left( \frac{L_N}{d} \right)^2 - 1 \right)$  (equ. 3.20) from ESDU 77028 table 8.1

$C_{Pa}$  is the boattail planform area coefficient. Note that we set this to 1.0 for the moment, i.e. we ignore the shape of the boattail for now and just assume it's cylindrical. This collapses the boat-tail planform area term, reducing equation 3.18 to:

$$C_{PL} = C_{Pf} \frac{L_N}{L} + \frac{L_m + L_T}{L} \quad (\text{equ. 3.21})$$

Forebody centre of pressure at finite angle of attack

To calculate the centre of pressure of the two forebody lifts at angle of attack, we'll use an extension of equation 3.11 to account for angle of attack:

$$\frac{X}{d} = - \frac{C_{m\alpha}}{C_{N\alpha}} \quad (\text{equ. 3.22})$$

so now we need an equation for  $C_{m\alpha}$ , the pitching moment about the nosetip at angle of attack. This is given in ESDU sheet 89014 as:

$$C_m = C_{m\alpha 0} \sin \alpha \cos \alpha - \frac{2}{\pi} \left( \frac{L}{d} \right)^2 C_{NC} C_{PL} C_{CL} \quad (\text{equ. 3.23})$$

Which again we'll split into its two parts:

$$C_{mfore} = C_{m\alpha 0} \sin \alpha \cos \alpha \quad (\text{equ. 3.24})$$

$$C_{mcrossflow} = - \frac{2}{\pi} \left( \frac{L}{d} \right)^2 C_{NC} C_{PL} C_{CL} \quad (\text{equ. 3.25})$$

Where  $C_{m\alpha 0}$  is the pitching moment coefficient about the nosetip at zero angle of attack, which we can get it by rearranging equation 3.11 as:

$$C_{m\alpha 0} = -C_{N\alpha 0} \frac{X_{nose\_alpha 0}}{d} \quad (\text{per radian}) \quad (\text{equ. 3.26})$$

where  $C_{N\alpha 0}$  is the lift curve slope at zero angle of attack that we got earlier from ESDU 89008 and  $X_{nose\_alpha 0}$  is the zero-angle of attack centre of pressure we got earlier from ESDU 89008.

Now we use equation 3.11 to divide equation 3.24 by equation 3.15 and we simply get:

$$\frac{X_{nose\_alpha}}{d} = \frac{X_{nose\_alpha 0}}{d} \quad (\text{equ. 3.27})$$





or in other words, the centre of pressure at angle of attack remains in the same position as the zero angle of attack position, it doesn't vary with angle of attack.

I'm not sure I believe that, and ESDU 89014 does say there was tentative, though suspect, evidence in the windtunnel data that the centre of pressure did move in the **transonic zone**. Fortunately, we're only concerned with angles of attack at low subsonic airspeeds.

For the second crossflow term, again, we use equation 3.11 to divide equation 3.25 by equation 3.16 and we get:

$$X_{crossflow} = \frac{L}{2} C_{CL} \quad (\text{equ. 3.28})$$

$C_{CL}$  is yet another geometric parameter: the *centroid of planform area coefficient*, or in other words, ESDU reckon that the cross flow centre of pressure is at the centre of planform area of the combined nosecone and cylindrical fuselage.

$C_{CL}$  is a fixed number, so again, ESDU reckon that the centre of pressure of the cross flow term doesn't move with angle of attack. Hmm...

To use (equ. 3.28) we need  $C_{CL}$  which again we get from EDU 77028, though not easily!

$$C_{CL} = \frac{C_{P_{f}}}{C_{P_L}} C_{c_f} \left(\frac{L_N}{L}\right)^2 + \frac{1}{C_{P_L}} \frac{L_m}{L} \left(\frac{L_m}{L} + 2\frac{L_N}{L}\right) + \frac{C_{P_a} L_T}{C_{P_L} L} \left(2 - C_{c_a} \frac{L_T}{L}\right) \quad (\text{equ. 3.29})$$

$C_{P_L}$ ,  $C_{P_f}$ , and  $C_{P_a}$  we derived earlier, and again we set  $C_{P_a}$  equal to 1.0

$C_{c_f}$  is the nosecone centroid of planform area coefficient which for a tangent ogive is equal to:

$$C_{C_f} = \frac{1}{C_{P_f}} \left( \frac{(F+1)^2}{\sqrt{2F+1}} \sin^{-1} \left( \frac{\sqrt{2F+1}}{F+1} \right) - \frac{2}{2F+1} \left( F^2 + F + \frac{1}{3} \right) \right) \quad (\text{equ. 3.30})$$

from ESDU 77028 appendix A5.3

where as before,  $F = \frac{1}{2} \left( 4 \left( \frac{L_N}{d} \right)^2 - 1 \right)$  from ESDU 77028 table 8.1

Again, we assume that the fuselage hasn't yet been boat-tailed, so that from ESDU 77028 appendix A.9 the boat-tail centroid of planform area coefficient  $C_{c_a} = 1.0$  which collapses the last term of equation 3.29 ( $C_{p_a} = 1.0$ )

Multiplying out the brackets gives:

$$C_{CL} = \frac{1}{C_{P_L}} \left( C_{P_f} C_{c_f} \left(\frac{L_N}{L}\right)^2 + \left(\frac{L_m}{L}\right)^2 + 2\frac{L_m L_N}{L^2} + 2\frac{L_T}{L} - \left(\frac{L_T}{L}\right)^2 \right) \quad (\text{equ. 3.31})$$

Note that the  $C_{p_f}$  term in equations 3.30 and 3.31 cancels out when you substitute 3.30 into 3.31



Boat-tailing: lift

Now that we (finally!) have the aerodynamics for a tangent-ogive forebody-cylinder combination, we can alter them to account for any boat-tailing.

ESDU sheet 87033 deals with conical boat-tails. There's rather too much unnecessary maths in there for our needs, as they strive to derive the combined lift and centre of pressure of the combination of forebody and boat-tail.

We, on the other hand, want to keep these two separate as we might want to use the results for a dynamic stability analysis where the angles of attack on forebody and boat-tail are different (see the 'stability' section later). This also removes the requirements for most of the maths in that ESDU sheet!

Having worked through the paper, the salient points are:

$$\text{Boat-tail lift: } C_{Nboat} = C_{N\alpha 0boat} \sin \alpha \cos \alpha (1 - \sin^{0.6} \alpha) \quad (\text{equ. 3.32})$$

$$\text{Where } \sin^{0.6} \alpha = (\sin \alpha)^{0.6}$$

**N.B.** software functions such as C++ `pow(x,y)` or Excel's `POWER()` can't compute a negative number raised to the power 0.6, they fall over and return gibberish, as the result is a complex number. So make the angle of attack always positive for the  $\sin^{0.6} \alpha$  term (the  $\sin \alpha$  term will sign the equation correctly).

The  $(1 - \sin^{0.6} \alpha)$  term is an attempt to match experimental data better, and is described as accounting for, among other things, the effects of separation of the flow over the leeward side of the boat-tail at angle of attack.

Equation 3.32 is again similar in form to equation 3.5, where  $C_{N\alpha 0boat}$  is the zero-angle of attack lift curve slope and is obtained from the equations given in figure 1 of that ESDU sheet: at subsonic speeds, the result for  $C_{N\alpha 0boat}$  is an equation identical to Barrowman's (equation 3.10 earlier) whereas at supersonic speeds the experimental (windtunnel) data has been curve-fitted to the following rather unwieldy equation:

$$C_{N\alpha 0boat} = \left(1 - \left(\frac{d_R}{d}\right)^2\right) (-0.6 - 1.4 \exp[A(M_\infty - 1)^{0.8}]) \quad (\text{per radian}) \quad (\text{equ. 3.33})$$

Where  $M_\infty$  is freestream Mach number,  $\exp$  is the natural exponential function  $e^x$ , and  $A$  is a geometry parameter:

$$A = -1.3 \left(\frac{L_T}{d}\right)^2 + 6.35 \left(\frac{L_T}{d}\right) - 7.85 \quad (\text{equ. 3.34})$$

Where  $L_T$  is the length of the boat-tail. The value of equation 3.33 diminishes with Mach number, the lift of the boat-tail changes to a less negative value.

Boat-tailing: centre of pressure

As for the centre of pressure, ESDU say it's halfway along the boat-tail for all Mach numbers and angles of attack, though this is just an estimate.

Actually, Barrowman's centre of pressure calculation (equ. 3.14) gives an answer that is nearly halfway along for moderate boat-tailing, so I suggest using it instead as it's more theoretically based.

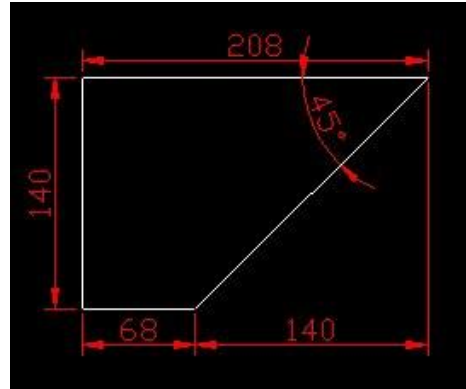
Fin lift at zero angle of attack

Unfortunately, the ESDU sheets that deal with fins are scarce on equations and big on complex graphs based on experimental results. And furthermore, you yourself often need to plot further graphs on a spreadsheet to interpret the results. This basically means that there's little mathematics I can give you.

The ESDU sheets do cover a wide range of fin shapes: **aspect ratio** and **taper ratio**, and various Mach numbers.

What we at Aspirespace decided to do was to design a fixed fin shape 'the aspire fin', get the ESDU data on it, and then use it on all our vehicles:

It's a typical rocketry fin shape, known as a cropped delta, and I'll give you the ESDU data on it so that you can decide whether or not you want to use it yourself. Just change the size of the fin (its planform area) to suit your own vehicle.



Now ESDU would regard this drawing to be of half a fin, the mirror-image other half isn't drawn. So two of our rocketry fins equals one ESDU fin.

The aspect ratio is 2.029 (assuming two rocketry fins side-by-side as per one ESDU fin), and the taper ratio is 0.327

The fin (planform) area is 19320 square units (per one rocketry fin or half an ESDU fin).

Fin subsonic data is given by ESDU 93034 and ESDU 95022, whilst supersonic data is given by ESDU 90013.

Again, we only need angle of attack data for low subsonic Mach numbers. At higher Mach numbers we only need the fin lift-curve slope at zero angle of attack, which is (ESDU 93034 fig 4 and ESDU 90013 fig 2):

Mach number	$C_{N\alpha 0}$ (per radian)
< 0.17	2.50
0.67	2.69
0.87	2.92
0.97	3.13
1.11	3.70
1.24	3.45
1.40	3.12
1.78	2.48
2.21	1.93
2.66	1.57
3.12	1.31
3.59	1.13
4.07	0.98
4.55	0.89
5.03	0.81
5.51	0.73
6.00	0.67

Note that these  $C_{N\alpha 0}$  values are for two fins angled at 180 degrees to each other round the fuselage. ESDU regards this as one complete (symmetrical) fin.



You can also regard this result as being applicable to four fins at 90 degrees to each other, two of the fins are assumed vertical so don't generate lift. I've ignored the values at exactly Mach 1 as they were extrapolated; there was no actual experimental data for the transonic zone.

Note also that the reference area for these values is the (planform) area of two rocketry fins (or one whole symmetrical ESDU fin), i.e. twice the fin area given above.

You should therefore re-reference these  $C_{N\alpha 0}$  values to the fuselage cross-sectional area by multiplying them by the factor:

$$\frac{\text{Fin planform area}}{\text{fuselage cross sectional area}} \quad (\text{equ. 3.35})$$

remembering that ESDU counts two fins as one whole fin.

When you do, you'll find that the zero-Mach  $C_{N\alpha 0}$  value is almost identical to Barrowman's result of equation 3.8 given earlier (within 1.5 percent) for four fins. This is well within the stated tolerance of the ESDU data.

#### Fin lift at finite angle of attack

The lift curve at subsonic Mach numbers of 0.5 or less is given by ESDU 93034 fig. 1, for which you need to cross-plot with taper ratio (see the given example in the data sheet). For high angles of attack (> 20 degs) use appendix A of ESDU 93034.

The resulting low subsonic (Mach less than 0.5) lift curve for our Aspire fin is:

Angle of attack (degs)	$C_N$
0	0
2	0.09
5	0.23
10	0.49
15	0.72
20	0.94
25	1.22
30	1.39
35	1.48
40	1.34
45	1.13
50	1.08

Note that for the value at 2 degrees, I multiplied the  $C_{N\alpha 0}$  value given earlier by two degrees (converted to radians).

Again, this data is referenced to the area of two fins (one symmetrical ESDU fin) and again you have to multiply by the factor given in equation 3.35 to re-reference to fuselage cross-sectional area.

Note also that the lift reaches a peak at 35 degrees angle of attack then reduces somewhat.



Three fins

The above data is for two or four fins (one or two ESDU fins) spaced equally around the circumference of the fuselage.

But what if you're using three equally spaced rocketry fins?

Barrowman calculated a correction factor for three fins which you multiply the four-fins value by.

Note that in his popular paper (Ref. 1) he derives a correction factor of  $\frac{\sqrt{3}}{2}$  but then crosses this out and uses a correction factor of  $\frac{3}{4}$

This is explained in his other paper (Ref. 2) by the fact that he simply forgot to square the  $\frac{\sqrt{3}}{2}$  factor, the correct factor is indeed simply  $\frac{3}{4}$

Fins centre of pressure

Subsonic values are given by ESDU 95022 (Figs 3, 4, and 5), and supersonic values are given by ESDU 90013.

For the fins, their centre of pressure varies with angle of attack, which is an added complexity: in a standard 4 fin arrangement, the two pitch fins may be at a separate angle of attack to the two yaw fins.

The ESDU values are given below as:  $\frac{X_{Fins}}{\text{root chord length}}$

measured aft of the leading edge position of the fin root chord. So add the distance of this point from the nosetip.

Mach	Angle of attack (degrees)						
	0	5	10	15	20	25	30
< 0.17	0.47	0.48	0.49	0.50	0.51	0.52	0.52
0.67	0.47	0.49	0.50	0.51	0.52	0.53	0.53
0.87	0.47	0.48					
0.97	0.46	0.48					
1.03	0.50	0.56					
1.11	0.54	0.59					
1.24	0.57	0.60					
1.40	0.59	0.61					
1.78	0.61	0.62					
2.21	0.63	0.63					
2.66	0.63	0.64					
3.12	0.63	0.64					
3.59	0.63	0.64					
4.07	0.64	0.64					
4.55	0.64	0.64					
5.03	0.64	0.64					
5.51	0.64	0.64					
6.00	0.64	0.64					

Note that the value of 0.47 for zero degrees angle of attack and Mach less than 0.17 is nearly identical to the Barrowman result of 0.46 (within 2%) which is well within the stated ESDU data tolerance.



### Interference effects on lift

Now we have the lift of the forebody-fuselage-boattail body combination alone, and also the lift of the fins alone. Unfortunately, these can't simply be added together. The presence of the fuselage affects the wing lift, and the presence of the wing affects the body lift.

Reference 3 is a seminal NACA report that allows calculation of these interference effects, and both Barrowman and ESDU base their interference calculations on this report, so give essentially the same results but to different levels of complexity.

Barrowman notes the two correction factors:

$K_{T(B)}$  is the correction factor for the fins lift in the presence of the body.

$K_{B(T)}$  is the correction factor for the body lift in the presence of the tailfins.

Barrowman notes that for typical rocketry fin sizes,  $K_{B(T)}$  is a small effect so he ignores it (sets it to zero), which is just as well as its derivation is highly complex (see below). He also notes that  $K_{T(B)}$  is practically linear with the ratio of fuselage radius over (net) fin span; this leads to his equation 3.9 given earlier:

$$K_{T(B)} = 1 + \frac{r}{s+r} \quad (\text{equ. 3.9})$$

Where this 's' is fin span (ESDU net semi-span) i.e. fin tip chord to fin root chord.

He also notes that the centre of pressure of the fins is not affected by the presence of the body.

ESDU goes into this in considerably more detail: ESDU 91007 again uses the same two interference factors (although it uses the subscript 'W' instead of 'T') which lets us derive the equations for the fin lift, and the carry-over of fin lift onto the body.

We'll treat these as separate entities as we may want to perform a stability analysis later, and these two have different centres of pressure.

$$C_{N\alpha 0\_fins\_corrected} = K_{T(B)} C_{N\alpha 0\_fins} \quad (\text{equ. 3.36}) \quad (\text{per radian})$$

$$C_{N\_fins\_corrected} = K_{T(B)} C_{N\_fins} \quad (\text{equ. 3.37})$$

$$C_{N\alpha 0\_carry\_over\_onto\_body} = K_{B(T)} C_{N\alpha 0\_fins} \quad (\text{equ. 3.38}) \quad (\text{per radian})$$

$$C_{N\_carry\_over\_onto\_body} = K_{B(T)} C_{N\_fins} \quad (\text{equ. 3.39})$$

Now we must remember to use the correct reference areas: we must have already re-referenced the fins from their planform area to the fuselage cross sectional area as discussed earlier (using equation 3.35) so that we can combine the lifts of the fins and fuselage later on.

ESDU confuses this issue somewhat by referring to the 'gross wing area' as that of the fin assuming the fin extends into the fuselage right to the fuselage centre line. The basic planform area we've been using all along (fin stops at the fuselage) ESDU calls the 'net wing area'.

Note that equations 3.36 to 3.39 are the same for Barrowman's method: he sets  $K_{B(T)}$  equal to zero.

Now comes the tricky bit: ESDU 91007 gives equations for  $K_{T(B)}$  and  $K_{B(T)}$  in Appendix A, and they're horrible!

Fortunately, it gives a graph of  $K_{T(B)}$ , from which I've derived an ESDU correction for Barrowman's equation 3.9:

$$K_{T(B)} = 1 + A \left( \frac{r}{s+r} \right) \quad (\text{equ. 3.40})$$

Where A is:

$\frac{r}{s+r}$	A
0.00	1.00
0.02	0.90
0.10	0.79
0.20	0.80
0.35	0.85
0.50	0.90
0.65	0.93
0.80	0.97
0.90	0.99
1.00	1.00

Now for subsonic speeds and low supersonic speeds,  $K_{T(B)}$  and  $K_{B(T)}$  are related by a simple formula (where I've converted ESDU's 'gross' semispan into our 'net' fin span):

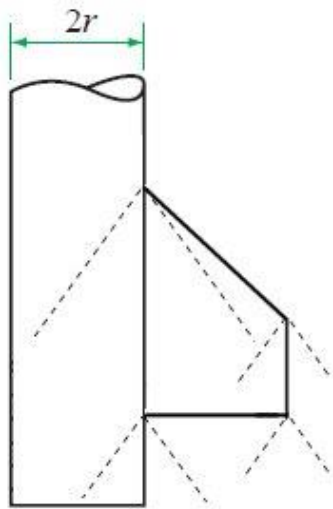
$$K_{T(B)} + K_{B(T)} = \left( 1 + \frac{r}{s+r} \right)^2 \quad (\text{equ. 3.41})$$

**N.B.** Note how this differs from equation 3.9, it's equation 3.9 squared. This is the first time that Barrowman's analysis has differed considerably from ESDU.

ESDU is saying that the fins lift (plus lift carry-over) is about 30 percent greater than Barrowman's analysis (which neglects the fins lift carry-over). Barrowman does note that his equation 3.9 is rather conservative (he uses a different equation in Ref. 2). This will have an effect on the vehicle's stability which we'll discuss in the later section on stability.

However, as the Mach number increases, it all gets very ugly:

Mach waves are essentially vanishingly weak shockwaves that radiate out from the corners of the fin (and are denoted on diagrams by 'Mach lines').



They have no strength of their own, but they demark a boundary where the airflow properties (pressure, speed, direction) can suddenly, albeit slightly, change. Or to put it another way it can show which areas of the fin are in subsonic flow, and which bits are in supersonic flow.

Where the Mach waves go therefore affects the overall lift of the wing and body. The lift of the fins gets 'carried over' onto the rear of the body in a region marked out by the Mach waves.

The angle of these Mach waves changes with Mach number, getting more acute as Mach number increases, so the effects are Mach number dependent.

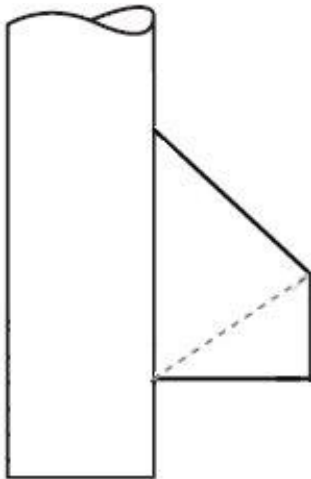
Burt Rutan's Spaceship One and Spaceship Two designs worry about the sudden flow changes caused by

Mach waves (and shockwaves), which is why you'll notice he's rounded all the corners off of his fins.

The effects of moving Mach lines on the lift of the fins alone has already been taken care of within the data of ESDU 90013 which we used earlier.

However, the effects of fin lift carried over onto the body have yet to be catered for; these are dealt with as a variation of  $K_{B(T)}$  with Mach number.

As long as the Mach number is low enough that the Mach line radiating from the upper fin tip hits the body within the length of the root chord all is well, and we can use simple equation 3.41



Unfortunately, as the Mach number increases, the point where this Mach line hits the body moves downstream: after it's reached the fin root chord trailing edge, the equations for  $K_{B(T)}$  get truly horrible, even in graphical form.

The Mach number where it hits the fin trailing edge is:

$$\beta + \tan(\text{leading edge sweepback angle}) = \frac{C_R}{S}$$

(equ. 3.42)

Where  $\beta$  is the supersonic similarity parameter  $\sqrt{M_\infty^2 - 1}$   
Rearranging gives:

$$M = \sqrt{\left(\frac{C_R}{S} - \tan(\text{leading edge sweepback angle})\right)^2 + 1}$$

(equ. 3.43)

Where  $C_R$  = root chord and  $s$  is fin span (ESDU net semi-span)

For our Aspirespace fin, equation 3.41 gives a Mach number of  $M = 1.1117$ , so above this Mach the equations for  $K_{B(T)}$  get onerous: if you can program the horrendously lengthy equations given in ESDU 91007 appendix A5 without making a mistake then you're a better programmer than I!

The equations are given in graphical form as graphs 2a to 2e of that paper, but are still hard work. Barrowman plots a simplified version of them in Ref. 2, I leave it up to you to decide whether to use his simplified graph or the following, bearing in mind that  $K_{B(T)}$  is a small effect.

The following three data tables for our Aspire fin are taken from the ESDU graphs for  $K_{B(T)}$ :

Graph 2a:

Mach number	$\frac{\text{body diameter}}{\text{fin root chord}}$						
	0.25	0.50	0.75	1.00	1.25	1.50	1.75
1.1117	3.8	3.2	2.6	2.3	2.0	1.7	1.5
1.2	3.4	2.6	2.2	1.8	1.5	1.2	1.1
1.4	2.6	1.9	1.5	1.2	1.0	0.8	0.6
2.2	1.2	0.7	0.5	0.3	0.3	0.2	0.2
3.5	0.7	0.3	0.2	0.1	0.1	0.1	0.1
5.0	0.3	0.1	0.1	0.1	0.1	0.1	0.1





Graph 2c:

	$\frac{\text{body diameter}}{\text{fin root chord}}$						
Mach number	0.25	0.50	0.75	1.00	1.25	1.50	1.75
1.1117	3.9	3.6	3.2	2.9	2.7	2.6	2.4
1.2	3.6	3.1	2.8	2.5	2.4	2.2	2.0
1.4	2.9	2.5	2.2	1.9	1.8	1.6	1.5
2.2	1.6	1.2	1.1	0.9	0.8	0.8	0.7
3.5	0.9	0.7	0.5	0.5	0.4	0.4	0.4
5.0	0.6	0.4	0.3	0.3	0.3	0.3	0.3

Graph 2e:

	$\frac{\text{body diameter}}{\text{fin root chord}}$						
Mach number	0.25	0.50	0.75	1.00	1.25	1.50	1.75
1.1117	4.2	3.8	3.5	3.2	3.0	2.9	2.7
1.2	3.7	3.3	3.0	2.8	2.6	2.5	2.4
1.4	3.1	2.7	2.4	2.2	2.2	2.0	1.9
2.2	1.7	1.4	1.3	1.2	1.1	1.0	1.0
3.5	1.0	0.8	0.7	0.7	0.6	0.6	0.6
5.0	0.7	0.5	0.5	0.5	0.5	0.5	0.5

Now each graph is for a different level of lift from the fins affecting the afterbody (the portion of the fuselage downstream of the fin trailing edge). The ESDU data is strictly for a non-tapering afterbody (no boat-tailing) but we'll use it for our boat-tail anyway in the absence of any other data.

Graph 2a is for no afterbody: the fuselage stops at the fins trailing edge.

Graph 2c is for a forebody 'length' of  $\frac{L_T}{2r\beta} = 0.5$  where  $L_T$  is the afterbody length,  $r$  is body radius, and  $\beta$  is the supersonic similarity parameter  $\sqrt{M_\infty^2 - 1}$

Graph 2e is for a forebody 'length' of  $\frac{L_T}{2r\beta}$  equal to or greater than 1.0

The values highlighted in green are where the data went off the edge of the graphs, but the graph curves were fairly flat by then anyway.

What you have to do is to calculate the parameter  $\frac{L_T}{2r\beta}$  for each Mach number given in the above tables, and then linearly interpolate the data from each table based on this parameter.

(The first data table 2a is for  $\frac{L_T}{2r\beta} = 0$ )

Then you have to divide the resulting number by  $C_{N\alpha 0\_fins} \left( \frac{s+r}{r} - 1 \right)$  to get  $K_{B(T)}$  (blame ESDU for this complexity). Note that you have to use the raw value of  $C_{N\alpha 0\_fins}$  (per radian) referenced to our fin area (two of our fins). I know, this is odd, as you'll then subsequently multiply  $K_{B(T)}$  by  $C_{N\alpha 0\_fins}$  re-referenced to fuselage cross-sectional area.



Interference effects on centre of pressure

The interference effects also affect the centres of pressure.

ESDU 92024 can be used to give the centre of pressure of the fins and the centre of pressure of the carry-over of the fin lift onto the rear of the body.

This ESDU sheet refers to the 'aerodynamic centre' rather than the centre of pressure, but at zero angle of attack the two are coincidental (equal), and this ESDU sheet only gives data for zero angle of attack. A brief discussion about the difference between the two terms is included at the end of the 'Stability' section of this document.

The centre of pressure of the fins remains unchanged by interference effects (as noted by Barrowman), but the derivation of  $\bar{X}_{B(T)}$ , the centre of pressure of the carry-over of fin lift onto the afterbody, is onerous, again lengthy equations occur.

Fortunately graphs are given, from which I've calculated the following tables for our Aspire fin:

**N.B.** As well as using the supersonic similarity parameter  $\beta = \sqrt{M_\infty^2 - 1}$  at supersonic speeds, this paper also uses the subsonic similarity parameter  $\beta = \sqrt{1 - M_\infty^2}$  at subsonic speeds.

Using figures 1 and 2 and appendix B2.1 of ESDU 92024, at subsonic speeds (Mach < 1)

$\frac{\bar{X}_{B(T)}}{C_R}$  is equal to:

Mach	$\frac{r}{s+r}$						
	0	0.05	0.1	0.2	0.3	0.5	0.8
0.0	0.271	0.310	0.329	0.355	0.372	0.397	0.433
0.3	0.273	0.310	0.330	0.354	0.370	0.395	0.430
0.5	0.277	0.312	0.330	0.353	0.368	0.391	0.424
0.7	0.285	0.315	0.331	0.351	0.364	0.384	0.412
0.8	0.292	0.318	0.332	0.349	0.360	0.378	0.402
0.9	0.303	0.323	0.333	0.346	0.355	0.368	0.386
0.95	0.311	0.326	0.334	0.344	0.350	0.360	0.374
0.97	0.317	0.328	0.334	0.342	0.347	0.355	0.366
1.0	0.337	0.337	0.337	0.337	0.337	0.337	0.337

where  $C_R$  is the fin root chord,  $r$  is fuselage radius, and  $s$  is our fin span (ESDU net semispan).



At supersonic speeds (Mach > 1.1117) ESDU 92024 figure 3 gives  $\frac{\bar{X}_{B(T)}}{C_R}$  as:

Table A

	$\frac{2r\beta}{C_R}$						
	0.1	0.25	0.5	1	2	3	4
$\frac{L_T}{2r\beta} = 0$	0.54	0.6	0.65	0.67	0.67	0.67	0.67
$\frac{L_T}{2r\beta} = 0.25$	0.56	0.63	0.7	0.8	0.92	1.02	1.14
$\frac{L_T}{2r\beta} = 0.5$	0.56	0.64	0.74	0.9	1.14	1.38	1.54
$\frac{L_T}{2r\beta} = 0.75$	0.58	0.68	0.78	0.97	1.32	1.62	1.92
$\frac{L_T}{2r\beta} \geq 1.0$	0.58	0.68	0.79	0.99	1.4	1.78	2.14

With this table, you have to first calculate the supersonic similarity parameter  $\beta = \sqrt{M_\infty^2 - 1}$  for increasing Mach number:

Mach	$\beta$	$\beta A$
1.1117	0.5	0.99
1.2	0.7	1.35
1.403	1.0	2.00
1.783	1.5	3.00
2.2	2.0	3.98
3.5	3.4	6.81
5	4.9	9.94

and then calculate parameters  $\frac{L_T}{2r\beta}$  and  $\frac{2r\beta}{C_R}$  where  $L_T$  is afterbody length,  $C_R$  is fin root chord.  $\beta A$  is  $\beta$  times the Aspire fin's aspect ratio.

Below a  $\beta A$  of 2, (highlighted in yellow) i.e. if the Mach number is less than 1.403 an interpolation has to be performed with the above table A to get a more correct  $\frac{\bar{X}_{B(T)}}{C_R}$

This interpolation is listed in appendix B2.2 of ESDU 92024. The interpolation results for two set Mach numbers are (note there's no beta in tables B and C):



Table B: Mach number = 1.1117

	$\frac{2r}{C_R}$						
	0.1	0.25	0.5	1	2	3	4
$\frac{L_T}{2r} = 0$	0.48	0.51	0.56	0.58	0.58	0.58	0.58
$\frac{L_T}{2r} = 0.25$	0.50	0.54	0.59	0.68	0.78	0.84	0.94
$\frac{L_T}{2r} = 0.5$	0.49	0.54	0.61	0.75	0.93	1.13	1.22
$\frac{L_T}{2r} = 0.75$	0.51	0.58	0.64	0.78	1.04	1.28	1.51
$\frac{L_T}{2r} \geq 1.0$	0.51	0.57	0.64	0.76	1.06	1.34	1.59

Table C: Mach number = 1.2

	$\frac{2r}{C_R}$						
	0.1	0.25	0.5	1	2	3	4
$\frac{L_T}{2r} = 0$	0.51	0.55	0.61	0.63	0.63	0.63	0.63
$\frac{L_T}{2r} = 0.25$	0.53	0.58	0.65	0.75	0.87	0.95	1.06
$\frac{L_T}{2r} = 0.5$	0.53	0.59	0.68	0.83	1.05	1.28	1.40
$\frac{L_T}{2r} = 0.75$	0.55	0.63	0.71	0.88	1.19	1.47	1.75
$\frac{L_T}{2r} \geq 1.0$	0.54	0.62	0.71	0.87	1.22	1.56	1.87

Linearly interpolate the results of all three tables (in the order: B,C,A) with increasing Mach number to get  $\bar{X}_{B(T)}$  if Mach number is less than 1.403 (i.e. set the values of table A to those at a Mach number of 1.403).

If Mach number is greater than 1.403, then you just use the results of table A.

If Mach number is greater than 1.0 but less than 1.1117, then linearly interpolate with Mach number between the subsonic values and the results of table B.

$\bar{X}_{B(T)}$  for all these graphs is measured aft of the fin root leading edge, so add the distance of this point from the nosetip.

Again, it's worth noting that these equations are for a cylindrical afterbody, but in the absence of any other data can be used for moderate boat-tailing (less than 10 degrees cone half-angle).

## 4: Stability

### Barrowman:

The basic stability of fixed-fin rocket vehicles at liftoff was calculated by James Barrowman using his lift and centre of pressure calculations listed earlier in section 3.


(Note that several books and web-pages contains errors in their reprinting of Barrowman's stability equations; it's better to get a copy of the original paper off the web: see Ref.1)

Barrowman's method is a classic static-stability analysis: it simply tells you whether your fins are large enough so that your vehicle has a tendency to keep the nose pointing in the direction of flight as required.

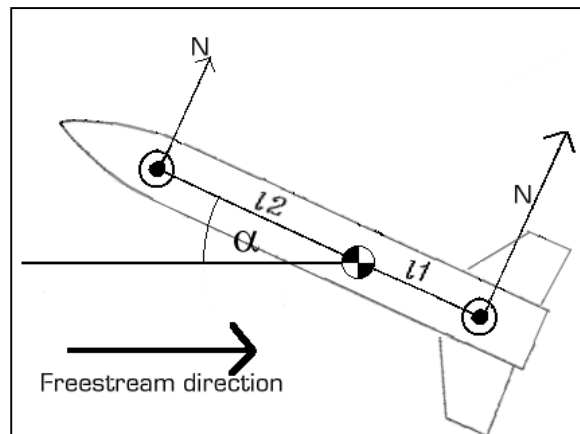
Static stability means that the effects on angles of attack at the nose and fins (and boat-tail) due to rotation of the vehicle about its CG is ignored: this rotation is assumed slow enough not to affect the analysis.

A dynamic stability analysis *does* include the effects of vehicle rotation, and will be discussed later.

### Static stability

Irrespective of whether or not the vehicle is translating, any rotation will naturally occur about the mass centroid (C of G, CG) which has symbol: 

Simply, a rocket vehicle is aerodynamically stable if it tends to reduce any angle of attack that might suddenly appear caused by a gust for example.



Taking the distance between CG and fins CP as  $l_1$ , and the distance between CG and forebody CP as  $l_2$  as shown:

The fins have to be sized so that their moment about the CG:  $N_{fins} l_1$  is greater than the forebody's moment about the CG:  $N_{forebody} l_2$  at whatever the value of angle of attack is.

The restoring moment  $M$  about the CG is then of course:

$N_{fins} l_1 - N_{forebody} l_2$  (equ. 4.1) and so a moment coefficient can be defined for this:

$$CM_{CG} = -\frac{CN_{fins} l_1 - CN_{forebody} l_2}{d} \quad (\text{equ. 4.2})$$

(therefore  $M_{CG} = qSd CM_{CG}$ ) (equ. 4.3)

The minus sign indicates that this 'restoring moment' opposes any increasing angle of attack for a stable rocket.

The  $d$  is a reference length used to make the moment coefficient dimensionless like the other aerodynamic coefficients; the fuselage diameter that was used to calculate the reference cross-sectional area is used as ' $d$ ' for consistency.

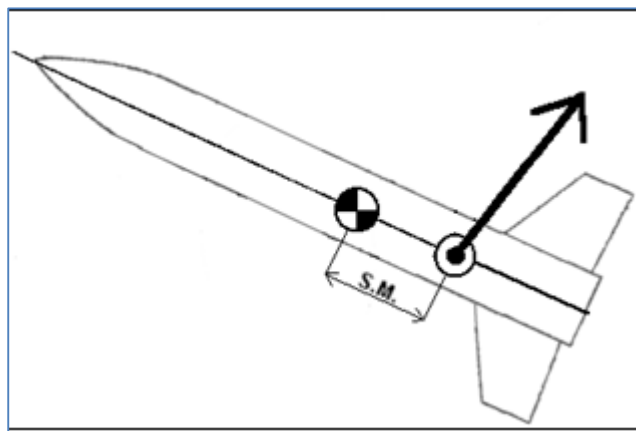
Lengths referenced as so many fuselage diameters are known as *calibres*.

There is a point along the fuselage about which the moment caused by the fins and forebody is zero. Barrowman calculates this overall centre of pressure by calculating the total aerodynamic moment about the nosetip, and then dividing this by the total lift.

Actually, he uses the coefficients:

$$\text{Overall centre of pressure} = \frac{C_{N\_forebody}X_{forebody} + C_{N\_fins}X_{fins} + C_{N\_boattail}X_{boattail}}{C_{N\_forebody} + C_{N\_fins} + C_{N\_boattail}} \quad (\text{equ. 4.4})$$

Barrowman then defines the degree of stability, or *Static Stability Margin* (often abbreviated to *Static Margin S.M.*) as the number of calibres that this overall centre of pressure lies rearwards of the CG. It should be around 1.5 calibres behind it.



Here's a table of suggested values from Ref. 5:

Suggested Static Margin (calibres)	1st stage	2nd stage
Dead calm	1.0 - 1.5	1.0
Windy	1.5 - 2.0	1.0
Encounters the Jetstream	2.0	2.0
Goes transonic	2.0	2.0
Very long, slender vehicle	Add 1.0	Add 1.0

The stability is referred to as the 'static' stability: this is because it is assumed that the vehicle rotates extremely slowly (technically infinitely slowly) about the CG, because a faster rotation rate causes further 'dynamic' effects discussed later.

Now as we've seen, the centre of pressure of the various parts of the vehicle (e.g. the fins) vary with angle of attack, and so the Static stability margin also varies with angle of attack.

Barrowman decided to remove this angle-of-attack variation by defining his static stability margin as that *at zero angle of attack* (actually assuming just an infinitesimal angle greater than zero) which he did by using the lift-curve slopes at zero angle of attack (recall that they are non-zero even at zero angle of attack). So:

Overall centre of pressure

$$= \frac{C_{N\alpha 0\_forebody}X_{forebody} + C_{N\alpha 0\_fins}X_{fins} + C_{N\alpha 0\_boattail}X_{boattail}}{C_{N\alpha 0\_forebody} + C_{N\alpha 0\_fins} + C_{N\alpha 0\_boattail}} \quad (\text{equ. 4.5})$$

Here  $X_{fins}$  is the fins centre of pressure at zero angle of attack.



We have a problem if we want to apply this equation to the ESDU-derived values, as we have two different components for the forebody.

So we simply total them up as:

$$\text{forebody centre of pressure} = \frac{C_{N\alpha 0\_forebody}X_{forebody} + C_{N\alpha 0\_crossflow}X_{crossflow}}{C_{N\alpha 0\_forebody} + C_{N\alpha 0\_crossflow}}$$

(equ. 4.6)

And:  $C_{N\alpha 0}$  for the forebody =  $C_{N\alpha 0\_forebody} + C_{N\alpha 0\_crossflow}$  (equ. 4.7)

Also remember to add the ESDU carry-over of the fin lift onto the afterbody, at its own centre of pressure  $X_{carry}$ , to equation 4.5:

Overall centre of pressure

$$= \frac{C_{N\alpha 0\_forebody}X_{forebody} + C_{N\alpha 0\_fins}X_{fins} + C_{N\alpha 0\_carry}X_{carry} + C_{N\alpha 0\_boattail}X_{boattail}}{C_{N\alpha 0\_forebody} + C_{N\alpha 0\_fins} + C_{N\alpha 0\_carry} + C_{N\alpha 0\_boattail}}$$

(equ. 4.8)

Aeroplane static stability

As an interesting digression: when analysing an aeroplane's static stability, the method is a little different.

The Lift vector acting at the wing centre of pressure is replaced by an equivalent system of Lift acting a little distance away from the centre of pressure plus a pitching moment.

This is done because when you analyse traditional straight wings, you can find a position for the Lift vector, (labelled the *Aerodynamic Centre AC*) where this AC doesn't move with angle of attack up to the wing stall. This is preferred to the centre of pressure because the center of pressure moves with angle of attack whereas the AC doesn't.

For symmetric aerofoils as used in rocketry, the aerodynamic centre and centre of pressure are effectively the same (coincidental), but only at zero angle of attack. As  $\alpha$  increases, the centre of pressure position moves rearwards from its limiting position at the aerodynamic centre at zero angle of attack, back to the centroid of planform area as  $\alpha$  approaches 90°.

Barrowman versus ESDU static stability

But back to rocket vehicles:

We've noted that ESDU equation 3.39 is the square of Barrowman's equation 3.9, ESDU's fins are lifting about 30% more than Barrowman's. This causes ESDU's static margin to be about 1 calibre more than Barrowman's at low airspeeds (which actually isn't much more).

At high subsonic airspeeds the discrepancy is larger, the ESDU analysis is giving yet more stability.

However, Barrowman's analysis, and our ESDU extensions to it, have assumed that the flow around the vehicle had zero viscosity (inviscid flow). As we'll see later in section 5, viscous flow effects actually move the CP forward, which reduces the static margin.



### One calibre

One calibre of Barrowman static stability has been found from trial and error to be a good minimum margin of static stability.

Why one calibre? Surely any fraction of a calibre that is greater than zero (CG ahead of CG) is stable?

However, as the angle of attack increases, the static stability significantly reduces, which is why a particularly strong gust can cause a rocket vehicle to tumble (have negative static stability) at liftoff. Having at least one calibre compensates for this.

Stability is reduced in the transonic zone, so investigate this speed range also: a large part of one calibre can vanish here. Our ESDU data is sketchy in the transonic zone.

### Dynamic stability

For details of how to compute a dynamic stability analysis see our paper 'A dynamic stability rocket simulator', excerpts from which are included below:

A faster rotation rate causes further 'dynamic' stability effects. The rotation is a pitch rotation, with positive pitch rate giving a nose-up rotation.

Reference 7 is a good attempt to analyse the dynamics of rocket flight, and I believe it forms the basis of dynamic analyses used by the excellent Rocksim software. However, Ref. 8 shows that an important feature is missing from that analysis, namely that the rocket vehicle is also able to move laterally as it rotates.

The effect of this extra degree of freedom is shown in Ref. 8 to increase the natural 'tail wagging' frequency and more importantly to increase the damping factor (see below): Reference 7 incorrectly assumes that vehicles with a high pitch moment of inertia will have near-zero rotational damping.

### Dynamic effects

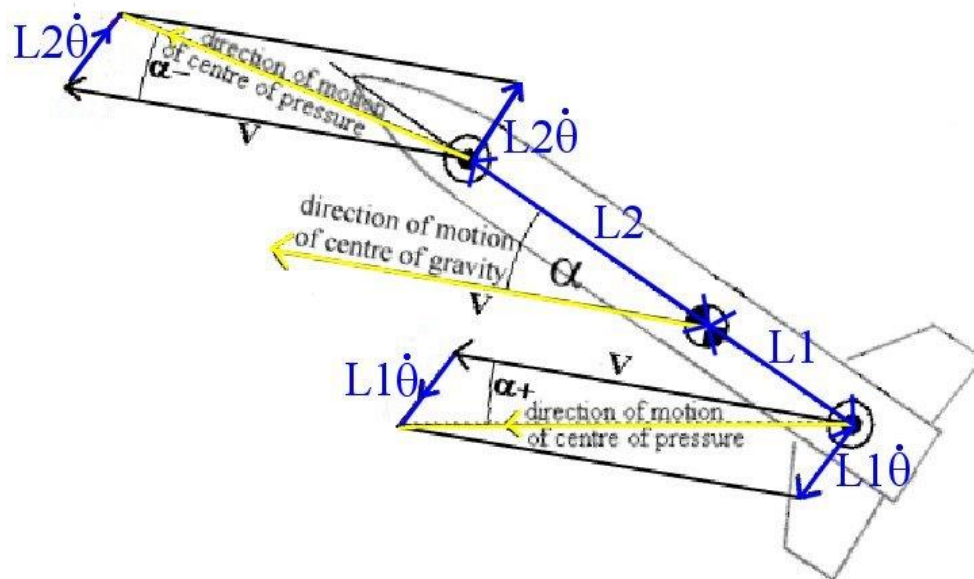
The Angle of attack on the nose, fin, (or boat-tail) is defined to be the angle between the incoming 'wind' and the long body axis of the vehicle (the axial axis, see section 2).

Up till now, we've assumed that the incoming 'wind' had the same direction all along the vehicle, so a general constant fuselage angle of attack ' $\alpha_{CG}$ ' was used to work out the various lifts.

However, if the vehicle is rotating in pitch (or yaw), the direction of the incoming 'wind' varies along the fuselage due to the rotation, so the angle of attack must vary along the fuselage too.



Here's a diagram of the ensuing velocity vectors:



A pitch-up rotation about the CG causes the fins to revolve with a velocity  $l_1\dot{\theta}$  where  $\dot{\theta}$  is the pitch rate, and the forebody similarly revolves with a velocity  $l_2\dot{\theta}$

Adding the airspeed vector  $V$  (of the CG), the velocity vector diagram above shows that the directions of motion (in yellow) of the fins and forebody are different to that of the motion direction of the C.G.

Remember that these directions of motion are exactly opposite to the directions of the incoming 'wind' at each point, so the angle of attack of the (centre of pressure of the) forebody is reduced by an amount  $\alpha-$  as shown, whereas the fins (and boat-tail) angles of attack are increased by an amount  $\alpha+$

This is why in section 3 I broke the lift of the vehicle up into separate lifts all at separate centres of pressure: they'll each have different angles of attack so must be computed separately in a dynamic analysis.

So rotating the vehicle nose-up reduces the lift on the nose, and increases the lift on the tailfins: this is an added stabilising effect that opposes the rotation, and is called *Aerodynamic damping*.

#### Aerodynamic damping

Let's investigate this damping mathematically.

Firstly, we'll assume that the extra angles of attack are small, so that we can use small angle approximations:

$$\cos(\alpha) \approx 1, \quad \sin(\alpha) \approx \tan(\alpha) \approx \alpha \quad (\text{radians})$$

It can further be assumed that for small angle of attacks the centre of pressures (CPs) of the fins and forebody don't move appreciably with angle of attack, so that  $l_1$  and  $l_2$  can be assumed fixed.

(They will slowly change with time due to movement of the CG as propellant is expelled out the rocket nozzle.)



Furthermore, if we assume that  $\alpha_{CG}$  is small (which assumes that the vehicle left the launcher with a goodly airspeed before being hit side-on by the wind) then the blue rotation vectors in the above picture become less skewed (more of a right-angle) to the velocity vector  $V$ .

With all of these assumptions, the extra 'dynamic' angles of attack are simply

$$\alpha^+ = \frac{l_1 \dot{\theta}}{V} \quad \alpha^- = \frac{l_2 \dot{\theta}}{V} \quad (\text{equ. 4.9})$$

where  $V$  is the vehicle's airspeed. (use  $l_3$  for the boat-tail)

Note that at the moment of liftoff, or at apogee on an exactly vertical flight, then  $V$  will be either zero or very small. This will cause either a divide-by-zero error on a computer, or if  $V$  is very small will make the dynamic angles of attack huge. To prevent these, limit  $V$  to be always greater than or equal to 1.0 in equations 4.9

To work out the main 'static' angle of attack  $\alpha_{CG}$  we'll split the incoming air into two components aligned with the Normal ( $Vv$ ) and Axial ( $Vu$ ) body axes direction (see section 2).

$$\text{So: } \alpha_{CG} = \tan^{-1} \left( \frac{Vv}{Vu} \right) \quad (\text{equ. 4.10})$$

The resulting angle of attack on the forebody is then:

$$\alpha_{fore} = \tan^{-1} \left( \frac{Vv}{Vu} \right) - \frac{l_2 \dot{\theta}}{V} \quad (\text{equ. 4.11})$$

And on the fins is:

$$\alpha_{fins} = \tan^{-1} \left( \frac{Vv}{Vu} \right) + \frac{l_1 \dot{\theta}}{V} \quad (\text{equ. 4.12})$$

And on the boat-tail is:

$$\alpha_{boat} = \tan^{-1} \left( \frac{Vv}{Vu} \right) + \frac{l_3 \dot{\theta}}{V} \quad (\text{equ. 4.13})$$

And so on, for the various lift components from the ESDU analysis of section 3.

Though the carry-over of fin lift onto the afterbody has a different centre of pressure to the fins, it is generated by the same angle of attack at the fins, e.g. equation 4.12.

The lift coefficients of each component (Normal force coefficients) are then calculated by multiplying the respective angles of attack by the respective lift curve slopes from section 3.

The total Normal (lift) force acting on the vehicle is then (omitting some lift components for the purpose of illustration):

$$N = \frac{1}{2} \rho V^2 S (CN_{forebody} + CN_{fins} + CN_{boattail}) \quad (\text{equ. 4.17})$$

These lifts (Normal forces) cause a pitching moment (+ve nose-up) about the C.G. which is:

$$M = \frac{1}{2} \rho V^2 S (CN_{forebody} l_2 - CN_{fins} l_1 - CN_{boattail} l_3) \quad (\text{equ. 4.18})$$

Note that we have a problem with the fins centre of pressure  $l_i$ : The fins centre of pressure given by the ESDU sheets actually depends upon fin angle of attack, but the added dynamic angle of attack on the fins depends upon the fin centre of pressure, it's a circular relationship.



Microsoft Excel will handle circular references, but you have to switch this ability on by going to the 'File' tab (or the 'Tools' option in older versions of Excel) then click 'Options', and then click 'Formulas'. In the 'Calculation options' section, select the 'Enable iterative calculation' check box.

In a trajectory simulator, this circular relationship would be handled by using the value of angle of attack from the last time iteration (last time round the calculation loop) to calculate the current centre of pressure, which then allows the calculation of angle of attack for the current time iteration.

Cross-spin force and damping moment

Recall equations 4.9:

$$\alpha^+ = \frac{l_1 \dot{\theta}}{V} \quad \alpha^- = \frac{l_2 \dot{\theta}}{V} \quad \text{where } V \text{ is the vehicle's airspeed.}$$

The lift that these equations (4.9) angles of attack cause are sometimes called the Cross-spin force coefficients CS (Ref. 6) although they aren't simple coefficients.

Note that as V is on the denominator of these fractions, then the faster the vehicle is flying, the smaller these extra angles of attack get, so the aerodynamic damping of rockets and aeroplanes decreases at high speed. This is why the pilots of Spaceship One had to be on their toes at high airspeeds of up to Mach 3!

You can formulate similar equations for damping in the roll axis, which again disappears at high airspeeds, which is why high-altitude finned rocket vehicles tend to spin rapidly.

In our pitching moment equation above, the CN's include these 'dynamic' angles of attack. However, the moment caused by these angles of attack alone are often treated separately: In Ref. 7 for example, equations (4.9) are used to create a separate moment about the centre of gravity of the vehicle called the Damping moment coefficient C2A, or damping moment CH (Ref. 6). Again, it isn't actually a coefficient.

From equ.s (4.9), the damping moment is:

$$CH = \frac{1}{2} \rho V^2 S \left( l_1 CN_{\alpha fins} \frac{l_1 \dot{\theta}}{V} + l_2 CN_{\alpha forebody} \frac{l_2 \dot{\theta}}{V} + l_3 CN_{\alpha oattail} \frac{l_3 \dot{\theta}}{V} \right) \quad (\text{equ. 4.19})$$

$$= \frac{1}{2} \rho V S \dot{\theta} (l_1^2 CN_{\alpha fins} + l_2^2 CN_{\alpha forebody} + l_3^2 CN_{\alpha oattail}) \quad (\text{equ. 4.20})$$

But this is all rather a digression just to explain where equation (4.20) as used in Ref.7 comes from.

Evaluation

How do we evaluate the dynamic stability of our vehicle?

References 6 and 7 have a go analytically, but forget that the vehicle is free to move laterally, which severely denigrates their analysis.

The only way to do the analysis properly is to code the equations into a three-degree-of-freedom (X,Y, and pitch rotation) trajectory simulator, and throw a gust at it to generate angles of attack along the vehicle. See our paper 'A dynamic stability rocket simulator' on the Aspirespace website 'technical papers' page for how to do this.



## Technical papers

---

It's worth noting that a rocket vehicle (or infact any aircraft) can be statically stable but dynamically unstable. If the static stability margin is too small (even though it is positive) then the vehicle can be dynamically unstable: any pitch or yaw oscillations can build in amplitude with time (known as divergence) until the vehicle tumbles. This is another reason why Barrowman suggests at least one calibre of static stability.

## 5: The effect of viscosity

### The boundary Layer

The airflow, or **flowfield**, around the vehicle can be treated as split into two separate regions to simplify the flowfield mathematical model. The property of fluids known as **viscosity** determines a suitable division.

The flowfield flowing around a vehicle behaves as though it were inviscid (zero viscosity) *except* within an inner *Boundary layer* of air of a few millimetres thickness enveloping the vehicle, and touching the vehicle's skin. This boundary layer hugging the skin can be treated as if the vehicle were wearing a thick sock, with the attendant effect that the effective fuselage cross-sectional area or 'profile' is increased.

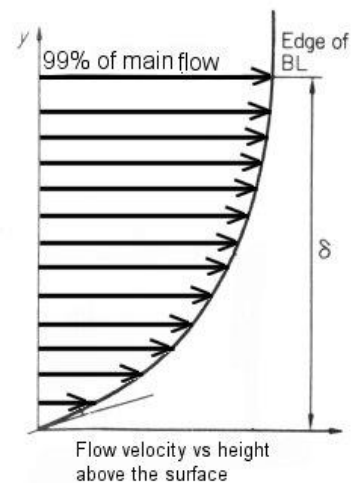
You can visualise a vertical slice through the Boundary Layer (BL) as a pack of cards lying on a table, where successive cards in the deck represent successive plane, parallel layers of air at increasing height above the skin of the vehicle (the table).

Throw the pack of cards onto the tabletop with a sideways motion, and the cards will begin to spread out due to friction with the tabletop.

This represents, in slow motion, the inviscid outer flowfield acting 'frictionally' on the edge of the boundary layer as it rushes past.

Note that successively lower cards in the pile move forwards with lower velocity; the lowest card remaining stationary on the table.

This is exactly how the layers of air within the boundary layer behave. Notice that the pack resists the forwards 'shearing' movement, due to the friction between each card and its neighbour, multiplied by the number of cards in the pack.



This is the source of *Viscous drag*, due to the (infinitely large) number of 'air layers' (of air molecules) sliding past each other.

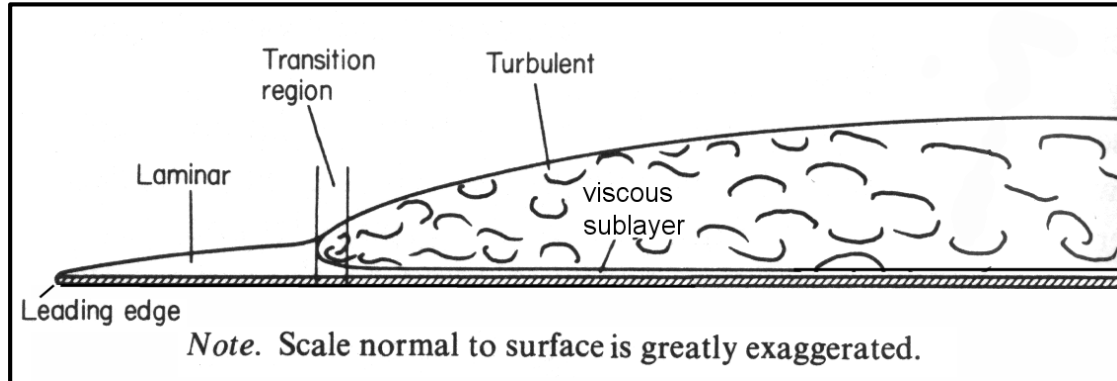
The lowest air layer sticks unmoving to the vehicle's skin. This is because, under a microscope, the skin surface is rough and irregular, so molecules of air bouncing off the many mountain peaks and valleys are scattered in every direction and bounce off their neighbours, giving an overall mean horizontal velocity of zero.

What is actually happening is that due to their random motion, molecules of air from one layer briefly impinge on the layer above. With their lower horizontal momentum, they are rear-ended by the faster moving molecules from the layer above, and the momentum exchange slows these faster moving molecules down, projecting the boundary layer out from the surface.

This nice, ordered mental picture of parallel layers, known as *Laminar flow* needs modified somewhat:

For one thing, the boundary layer gets thicker with distance along the surface. This is termed *Boundary layer growth*, and is caused by friction progressively slowing the horizontal velocity of each layer, which grows the boundary layer outwards from the top layer: more layers, (or cards), are added to the pile with increasing horizontal distance.

Also, at some point along the length of the vehicle the boundary layer breaks up. What determines this *Transition* to chaotic, or *Turbulent* behaviour isn't desperately well known, as chaos theory is still in its infancy, though there is quite a large empirical database on transition, even if there's a lack of theory.



As well as being thicker, a turbulent boundary layer causes more drag, because as well as the molecular transport of momentum between the layers that we saw with laminar flow, the eddies and whirlpools of the turbulence move large sashes of fluid between the layers, causing a larger momentum exchange. Ultimately, this energy exchange becomes waste heat. So we want to preserve the laminar flow as much as possible.

If the flow hits an obstacle, even as small as a rivet, the flow will trip to turbulent, which is why the skin of the vehicle must be very smooth, particularly at the front (forebody). A glassy-smooth finish on a composite forebody reduces the drag considerably below that for just a fairly good paint-job. Any step whatsoever at the joint between nosecone and fuselage will also trip the flow turbulent.

The boundary layer will 'trip' turbulent all by itself though, simply after having had to flow over the skin for a long enough period of time. Assuming the vehicle is accelerating slowly compared to 'aerodynamic time', this represents a critical length along the vehicle where the boundary layer will suddenly 'trip'.

Each extra millimetre travelled makes the boundary-layer less stable until it simply goes unstable. You can see this effect clearly in the smoke rising from a cigarette: the smoke is initially laminar, but after a critical distance above the cigarette it suddenly goes turbulent, breaking up into thick eddies.

Assuming a decent forebody finish, the point along the fuselage where transition to turbulent flow will occur can be estimated using a flow parameter known as the *Reynolds Number*, defined here as:

$$\frac{\rho V x}{\mu} \quad (\text{equ. 5.1})$$

where  $\rho$  is the air density (1.225 kg/m<sup>3</sup>),  $V$  is the freestream velocity (or vehicle airspeed),  $\mu$  is the viscosity of the air (18.2), and  $x$  is the axial distance the flow has travelled downstream of the nosetip.

Experience suggests that transition will occur when the Reynolds number is somewhere between 10<sup>5</sup> and 10<sup>6</sup>, and this is often towards the rear of the fuselage, so it is worth having a very smooth surface finish at least up to this point.

The boundary-layer will trip turbulent when it encounters the fins.



When the vehicle goes transonic (above about Mach 0.8), shockwaves will trip the boundary layer at the nose, usually where the curve of the nose meets the straight fuselage. The same applies for supersonic speeds.

The (displacement) thickness of the Boundary layer is classically defined as running from the vehicle skin to a point that has 99% of the main flowfield velocity above that section of skin, and it is typically a few millimetres thick at most, which is why small surface irregularities affect it so much.

**The viscous sublayer**

Transition notwithstanding, a smooth skin surface causes less viscous drag than a slightly rougher one. As viscous drag is typically 70 to 80 percent of the rocket vehicle drag, this difference is important.

The reason is interesting: at the bottom of the boundary layer is a thin layer known as the viscous sublayer (this is sometimes incorrectly called the laminar sub-layer: it isn't laminar, just has a laminar-like velocity profile). What distinguishes this region is that it's so close to the wall that turbulent mixing from the rest of the boundary layer above it is damped/suppressed by viscosity, so even if the boundary layer is turbulent, the flow in this sublayer remains at a very low speed.

So provided that the peaks of surface roughness don't protrude through the viscous sublayer, then the flow speed around the roughness obstacles remains near-zero, so the viscous drag doesn't increase.

But if the roughness extends above the sublayer, then the flow speed around the tops of the obstacles is no longer low, and the viscous drag then increases markedly.

**Viscous corrections**

Earlier, we used ESDU sheet 89008 to determine the lift of the forebody (nosecone plus forward fuselage) at zero angle of attack. This ESDU sheet also gives two viscous correction terms which are to be added to the forebody lift coefficient at zero angle of attack:

$$C_{Na0\_forebody}$$

The first viscous correction term accounts for the fact that the fuselage effectively gets fatter as the boundary layer grows in thickness along the body. This first term (equation 3.4 from that ESDU sheet) is equal to  $\frac{8}{d} \delta^*$  (equ. 5.2) where  $\delta^*$  is the thickness of the boundary layer at the tail end of the fuselage, and is given in figure 3 of that paper.

In tabular form, figure 3 is (thickness in millimetres divided by the body length L):

	LRe								
Mach number	5	5.5	6	6.5	7	7.5	8	8.5	9
0	4.58	3.74	2.99	2.35	1.89	1.52	1.25	1.01	0.81
0.5	4.75	3.90	3.16	2.51	2.06	1.68	1.36	1.11	0.89
1	5.27	4.41	3.60	2.90	2.31	1.86	1.52	1.23	1.00
1.5	6.10	5.16	4.26	3.47	2.80	2.27	1.85	1.51	1.21
2	7.03	5.93	4.90	4.07	3.34	2.68	2.17	1.75	1.42
2.5	8.00	6.73	5.63	4.67	3.88	3.18	2.60	2.14	1.73
3	8.90	7.57	6.39	5.32	4.36	3.60	2.96	2.44	2.01
3.5	9.60	8.25	7.05	5.91	4.88	4.02	3.34	2.77	2.26
4	10.30	8.85	7.57	6.42	5.39	4.48	3.71	3.08	2.51
4.5	11.10	9.60	8.20	6.99	5.89	4.88	4.06	3.36	2.76



5	12.00	10.30	8.80	7.51	6.28	5.25	4.40	3.66	3.02
---	-------	-------	------	------	------	------	------	------	------

Where LRe is the Log to base 10 (Log10) of the body Reynolds number, where the body Reynolds number is the Reynolds number based on the length of the vehicle (x is body length L in equ. 5.1)

Multiply the above values by 0.001 to get into metres, then multiply by the length of the vehicle 'L' to get the displacement thickness at the rear of the vehicle to insert into equation 5.2

The centre of pressure of this viscous term acts at the fuselage mid-point (L/2) where length L includes nosecone and boat-tail.

You'll need the results of a trajectory sim to calculate the Reynolds number, which alters with airspeed and altitude.

The second viscous term describes the boundary-layer contribution arising from the frictional force acting over the surface of the body as the airflow flows around the circumference of the fuselage at (slight) angle of attack.

Both of these corrections assume that the boundary layer is fully turbulent along the length of the body, which is a reasonable assumption for supersonic speeds and HPR sized rocket vehicles (but not for small model rockets).

This second term is equal to  $4C_F \frac{L}{d}$  (equ. 5.3) where  $C_F$  is the mean skin-friction coefficient (assuming a fully turbulent boundary layer) and is given in figure 4 of the ESDU paper. Vehicle length L includes nosecone and boat-tail.

In tabular form, figure 4 is:

Mach number	LRe								
	5	5.5	6	6.5	7	7.5	8	8.5	9
0	7.18	5.50	4.36	3.57	2.96	2.48	2.11	1.81	1.57
0.5	7.10	5.40	4.28	3.51	2.90	2.43	2.06	1.77	1.53
1	6.77	5.17	4.11	3.33	2.74	2.30	1.94	1.66	1.43
1.5	6.40	4.82	3.82	3.07	2.53	2.12	1.78	1.54	1.32
2	6.00	4.47	3.48	2.80	2.29	1.91	1.62	1.37	1.18
2.5	5.65	4.12	3.18	2.54	2.07	1.73	1.45	1.23	1.04
3	5.30	3.80	2.90	2.31	1.86	1.54	1.30	1.10	0.94
3.5	4.98	3.51	2.65	2.08	1.68	1.39	1.17	0.98	0.84
4	4.70	3.28	2.46	1.91	1.53	1.26	1.05	0.88	0.75
4.5	4.50	3.07	2.27	1.77	1.40	1.14	0.94	0.80	0.67
5	4.31	2.90	2.11	1.63	1.28	1.04	0.85	0.72	0.61

Divide the table entries by 1000 to get  $C_F$ .

Again, the centre of pressure of this viscous term acts at the fuselage mid-point (L/2) where length L includes nosecone and boat-tail.

ESDU 89008 suggests simply adding these terms to the inviscid  $C_{N\alpha 0}$  we got earlier, but for a dynamic stability analysis it's better to treat these two corrections as an entirely separate lift-curve slope for the cylindrical portion of the fuselage, and then apply them through the first term of equation 3.15 i.e.

$$\text{'fuselage lift'} = C_{Nfuselage} = C_{N\alpha 0 additions} \sin \alpha \cos \alpha \quad (\text{equ. 5.4})$$





ESDU 89008 suggests that these two corrections have centres of pressure at the body mid-length ( $L/2$ ) which is why it's better to deal with them separately from the inviscid lift.

Adding these two terms increases the nose lift, and both their centres of pressure are ahead of the overall vehicle centre of pressure. So these additional terms are destabilising, the overall centre of pressure gets moved forwards by them.

Boattail

There is also a viscous crossflow term for the boattail:

$$C_{Nboat} = C_{DC} \sin^2 \alpha \quad (\text{equ. 5.5})$$

Where  $\sin^2 \alpha = (\sin \alpha)^2$

$C_{DC}$  is the drag coefficient of 'cross flow' or flow around the circumference of the boat-tail at angle of attack.

A curve-fitted equation for  $C_{DC}$  is given in figure 2 of ESDU 87033. However, it depends upon the term  $M_\infty \sin \alpha$  which will always be small for our vehicles (near-zero Mach and moderate  $\alpha$ , or higher Mach and near-zero  $\alpha$ )

For small  $M_\infty \sin \alpha$  figure 2 says:

$$C_{DC} = -\left(\frac{L_T}{d}\right) \left(1 - \frac{d_R}{d}\right) \quad (\text{equ. 5.6})$$

where  $L_T$  is the boat-tail length and  $d_R$  is its smaller diameter.

Note that  $C_{Nboat}$  is negative for positive  $\alpha$ , but due to the squaring is still negative for negative  $\alpha$ .

That may be correct mathematically, however negative  $\alpha$  is an angle of attack in the opposite direction, so it should give lift in the opposite direction, i.e. make equation 5.6 positive for negative  $\alpha$  to make equation 5.5 positive for negative  $\alpha$ .

**Viscous effect on static stability**

We add the forebody viscous terms to the equation for forebody centre of pressure:

$$= \frac{C_{N\alpha0\_forebody}X_{forebody} + C_{N\alpha0\_crossflow}X_{crossflow} + C_{N\alpha0\_viscous\_terms}X_{viscous\_terms}}{C_{N\alpha0\_forebody} + C_{N\alpha0\_crossflow} + C_{N\alpha0\_viscous\_terms}} \quad (\text{equ. 5.7})$$

The viscous correction terms and the inviscid first term both use the same  $C_{N\alpha0}$  which is  $C_{N\alpha0\_forebody}$

For the boat-tail's contribution to stability, oddly we don't have to add the viscous term.

That's because it varies with  $\sin^2 \alpha$  (from equation 5.5) which from small-angle approximation theory ( $\sin \alpha = \alpha$ ) means that at near-zero  $\alpha$  the term varies with  $\alpha^2$  which gives the shape of a parabola.



Now a parabola has zero gradient at zero  $\alpha$ , so  $C_{N\alpha 0}$  for the boat-tail viscous term is zero, it doesn't get added to the static stability equation which is calculated at zero  $\alpha$ .

There are no viscous corrections for the fins. That's because the fins data already includes the effects of viscosity: the generation of vortices at non-zero angle of attack (which is further discussed in ESDU 91042, which I haven't used, in section 3).

When you add the viscous corrections to the inviscid ESDU static stability analysis from section 4, the static stability margin reduces, and infact is nearly identical to Barrowman's (inviscid) static margin result at launch, which is the reason why Barrowman's stability analysis remains effective: launch is often the critical stability portion of the flight for solid-motor powered vehicles.



## **6: Drag**

I've kept the calculation of rocket vehicle drag to last, as it depends heavily upon viscous drag, the shearing drag caused within the boundary layer.

The drag (axial) force is defined as:  $Drag = \frac{1}{2} \rho V^2 S C_D$  (equ. 6.1)

Where  $C_D$  is the drag coefficient, and  $S$  is the cross-sectional area of the fattest part of the fuselage.

### **The missing drag conundrum**

One can perform weeks of advanced ESDU data sheets drag analyses, (and we have) and you'll get a total fuselage plus fins drag coefficient (based on fuselage max cross-sectional area) that pretty well always comes out at a value close to  $C_D = 0.3$

Unfortunately, when you then fly the rocket-vehicle, you'll find that the average drag coefficient over the flight is actually around 0.5 subsonic and 0.6 supersonic, and nobody seems to know where the extra drag comes from.

The drag changes dramatically after motor burnout, so the extra drag seems to be caused by the large hole at the back after burnout.

But even the drag coefficient while the motor is still burning is larger than it should be: somehow the rocket exhaust is sucking on the air over the boat-tail, causing a low-pressure region over and behind the boat-tail that is sucking on the rear of the vehicle, slowing it down.

Basically, the Scots who performed all those experiments with augments ducts bolted to the boat-tail back in the 1930's knew what they were on about, changing this extra drag into thrust, but sadly, their data has been lost to antiquity.

It's very easy to extract drag data from actual flights what with all the modern accelerometer-based flight computers for sale nowadays (e.g. the RDAS), and the flight data from the actual rocket vehicle is as accurate as you will ever get anyway, so there's no need to perform vast pre-flight drag analyses anymore: simply lob the rocket vehicle, or a small model of it, on a lower-power motor to start with to get the drag data.

However, we'll explore aspects of the drag in the interests of education, and it's worth knowing how the drag breaks down into its component parts for structural calculations.

### **Overall estimate**

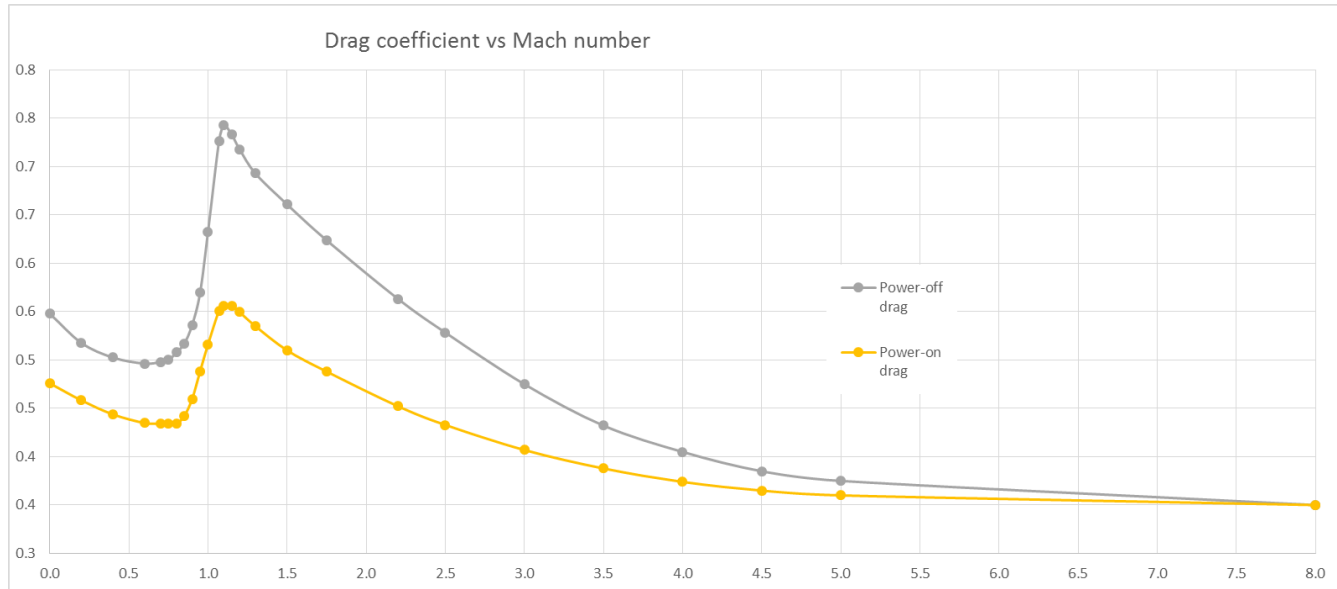
The other point about drag data is that it's easy to program trajectory sims with different drag coefficients to see what happens.

As a first ballpark estimate, subsonic drag coefficient for a typical rocket vehicle is around 0.5, whereas use 0.6 if it goes supersonic, no matter how briefly.

Note that the drag with the engine thrusting ('power-on') is lower than the drag with the engine off ('power-off').



As a better estimate, the following generic drag curve is an amalgam of drag curves from Aerolab, a Computerised Fluid Dynamics (CFD) package, plus several sounding rockets such as the Arcas Robin.



Mach	Power off Drag coefficient	Power on Drag coefficient
0.00	0.548	0.476
0.20	0.518	0.458
0.40	0.503	0.444
0.60	0.496	0.435
0.70	0.498	0.434
0.75	0.500	0.434
0.80	0.508	0.434
0.85	0.517	0.442
0.90	0.536	0.460
0.95	0.570	0.488
1.00	0.632	0.516
1.07	0.727	0.551
1.10	0.743	0.556
1.15	0.733	0.556
1.20	0.718	0.550
1.30	0.693	0.535
1.50	0.661	0.510
1.75	0.624	0.488
2.20	0.563	0.452
2.50	0.528	0.433
3.00	0.475	0.407
3.50	0.432	0.388
4.00	0.405	0.374
4.50	0.385	0.365
5.00	0.375	0.36
8.00	0.35	0.35



### **Skin-friction drag**

Note that boundary layer transition notwithstanding, a smooth skin surface causes less skin-friction drag than a slightly rougher one. As skin-friction drag is typically 70 to 80 percent of the rocket vehicle drag, this difference is important: polish the surface.

### **Boat-tailing**

Boat-tailing reduces drag, but at the expense of moving the centre of pressure of the vehicle forward, which reduces the Static stability margin, hence bigger fins are required, and hence larger fin-drag. If the boat-tailing is too excessive (a cone half-angle more than 10 degrees) the flow separates over the boat-tail which greatly increases the drag.

### **Base drag**

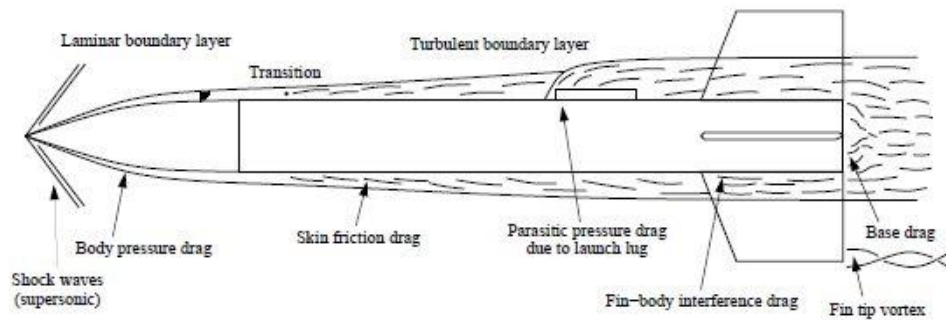
Rocket-vehicle fuselages tend to be squared-off at the back to accommodate the rocket engine nozzle/s. The fact that the fuselage then doesn't end in a sharp point like a teardrop causes extra drag, called base drag.

Unfortunately, base drag predictions tend to be wrong, usually way too low, especially when the rocket is firing. This is frankly because the whole notion of 'base drag' is woolly because there's no good way to isolate the portion of the drag that can be blamed on the base. Is the base drag supposed to be the difference between a pointy-ended fuselage and a squared-off one? If so, how do you uniquely define the pointy-ended shape? There's an infinite variety of pointy-end shapes you could put on.

Or, is the base drag caused by suction: the difference in the pressure over the base compared to ambient pressure? Unfortunately, there's no justifiable reason why ambient pressure should be the baseline pressure here.

### **Valid drag assumptions**

- The angle of attack is always small, so that the drag is insensitive to angle-of-attack effects, i.e. lift-induced drag caused by lift effects at angle of attack is ignored.
- There are five components of drag: *Skin-friction drag*, *Profile drag* (also known as *Form drag* or *Pressure drag*), supersonic *Wave drag*, *Base drag* at the rear of the vehicle, and *Excrescence drag*: the drag due to protuberances such as rail guides, cutouts, and conduits. (Confusingly, *Skin-friction drag* and *Form drag* added together is called *viscous drag* because without the viscous boundary layer and viscous wake, the *Form drag* would be zero.)
- Subsonic flow around the vehicle will be mostly turbulent, though there will probably be a region of laminar flow around the nose. You could assume that the flow is initially laminar and then trips into turbulence once the product of Unit Reynolds number times distance from the nosetip in metres exceeds about 10 to the power 6, or the flow crosses a roughness, slot, or protuberance. (Even a groove a few fractions of a millimetre can trip the flow turbulent.)
- Supersonic flow around the vehicle will be all turbulent due to nose-shockwaves tripping the boundary layer turbulent.
- Turbulent flow creates more drag than Laminar flow, so delay the onset of tripping to turbulence as much as possible by keeping the outer skin of the vehicle as smooth as possible (mirror- smooth is best, though not always practical.)
- Whether or not the boundary layer is laminar or turbulent, surface roughness increases skin-friction drag.
- The various drag components are simply added together to obtain the total drag, as is the usual aero industry practice for drag effects: no interference/upwash effects are included.



### Subsonic drag: Mach number < 0.8

#### Skin friction drag

ESDU data sheet 78019 can be used to calculate the drag of the forebody, and also the fins.

The skin-friction drag is taken from data for the drag on flat plates at zero angle of attack by Spalding and Chi, and assumes totally turbulent flow. Their methodology is presented within this data item as a best-fit formulae for Mach < 0.9 accurate to within 0.1%. Correction formulae for areas of laminar flow (using Blasius' boundary-layer model) are included.

The flat-plate skin-friction drag models used in this paper can be used directly to calculate the skin-friction drag of the fins. Don't forget that each fin has *two surfaces*.

The flat-plate skin-friction drag result has been factored by 1.05 to take account of the 3-D flow effects due to the nosecone curvature.

Remember that skin friction drag is referenced to skin area; you'll need to convert to add it to other drag components using the factor:

$$\frac{\text{fuselage cross-sectional area}}{\text{skin area}}$$

#### Profile drag

This same data item ESDU 78019 also gives formulae for calculating the profile drag of the forebody as a factor of the skin-friction drag. (This works because the profile drag is much less than the skin-friction drag.)

This paper assumes that a short boat-tail completely closes the rear, so for rocket-vehicles with the inevitable squared-off end, an extra drag term must be added (see base drag below).

Fin profile drag data for typical rocket-vehicle thin fin shapes is scarce, but estimates can be obtained from ESDU item Wings.02.04.03 which deals with the subsonic drag of round-nosed subsonic sections

An alternative is the textbook 'Fluid dynamic drag' by Hoerner, which also has subsonic fin data, or try the internet.

#### Base drag

The drag of the rear of the fuselage, or Base region, strictly depends upon whether the motor is burning or not, as its exhaust interacts with the flow around the base.

Power-off drag (i.e. the motor is not burning) for a blunt base can be obtained from ESDU 76033 as the near-constant value 0.14, whereas the power-off drag of a boat-tailed base can be found from ESDU 76033 and 77020 in combination.



Power-on base drag data might possibly be obtained via the Web, but if not, use the difference between power-on and power-off drag in the above graph.

Note the above caution that base drag coefficient turns out to be 0.2 higher in practice, for reasons unknown.

Excrescence drag

Increase the total drag by 10% to account for excrescences as is usually done in practice.

**The Transonic zone:  $0.8 < \text{Mach number} < 1.2$  (ish)**

Accurate prediction of transonic drag is sadly a current state-of-the-art problem in Computerised Fluid Dynamics analyses.

Base drag

The base drag is obtained from the same source as its subsonic calculation, though Power-off data for blunt rears and also boat-tails exists in ESDU 78041

Excrescence drag

Increase the total drag by 20% to account for excrescences as is usually done in practice at Supersonic speeds.

**Supersonic drag:  $1.2 > \text{Mach number} > 5$ ish**

Skin friction drag

Yet again, the method of Spalding and Chi used for the subsonic calculations is the most appropriate.

ESDU 73016 lists their method, though for higher accuracy, their corrections for boundary-layer thermal heating at higher Mach numbers should be incorporated.

The drag coefficients are calculated using a Reynolds number based on an appropriate streamwise length: body length for the body, and mean geometric chord for the fins. The drag of the various surface areas are then normalised to the cross-sectional area of the fuselage.

The drag of the nosecone is factored by 1.05 as advised, to correct their flat-plate model for 3-dimensional flow effects.

Wave and Profile drag

Relevant ESDU data sheets on the drag of forebodies exist, such as ESDU B.5.02.03.04 or ESDU B.5.02.03.06

Fin wave drag data can be obtained from ESDU item 75004.

The drag increment due to blunted leading edges can be obtained from the textbook 'Fluid dynamic drag' by Hoerner.

Base drag

The power-off base pressure acting on the rear of a 'squared-off' fuselage can be read directly from the graph in ESDU item Bodies.S.02.03.12 which deals with this issue, and the drag is simply the negative of this pressure.

The power-on base drag can be obtained from the same source as its subsonic calculation.



## Technical papers

---

### Excrescence drag

Increase the total drag by 15% to account for excrescences as is usually done in practice.





## 7: Measuring the aerodynamic coefficients

It is very difficult to either pre-predict or measure any of the aerodynamic coefficients correct to better than 10 percent. Such a lack of precision is characteristic of aerodynamic data.

The coefficients  $C_D$  and  $CM_{CG}$  are sometimes determined by measurements taken during flight.

To determine  $C_D$  one makes accurate measurements of the deceleration of the rocket in flight after burnout using accelerometer data.

### Aerodynamic damping

In section 4, I introduced the concept of aerodynamic damping; a damping of the pitching motion of the vehicle due to pitch-rate-induced 'damping' angles of attack. (Pitch rate is rotational velocity in radians per second).

Now the pitch-rate-induced angle of attack is different all along the fuselage as it depends upon distance from the vehicle's C.G. This means that you'd need to integrate its effect all along the fuselage.

We simplify this integration by selecting particular angles of attack at the centre of pressure of the various components (forebody, fins, boat-tail, etc) but it must be borne in mind that this isn't nearly as exact as proper integration: the real aerodynamic damping may well be larger.

To get the correct aerodynamic damping coefficient  $CM_{CG}$  we need to analyse the pitching motion of the vehicle, in particular the pitching moment at the vehicle CG:

### Measurement of $CM_{CG}$ : the 'wavelength of yaw'

HPR rocket vehicles with reasonable static stability are lightly damped, so they oscillate in pitch (and yaw) throughout their trajectory by a degree or so.

This angle of attack wiggling is small enough that the trajectory can be approximated for simulation purposes as if there was no wiggling.

Back in the early days of ballistics, (Ref. 6) the complete lack of digital computers meant that a great deal of simplification of the equations of motion of a flying rocket vehicle were necessary to allow hand-calculation. (See our companion paper 'A dynamic stability rocket simulator' on the Aspirespace website 'technical papers' page).

While nowadays we numerically integrate the simulated trajectory with respect to time, they integrated small-angle of attack approximation formulae with respect to distance along the trajectory, for obscure mathematical reasons that I won't repeat here.

One resulting formula is called 'the wavelength of yaw' (or pitch) and describes the actual distance in metres travelled along the flightpath between the peaks of successive wiggles:

$$\text{wavelength } \sigma = 2\pi \sqrt{\frac{I}{\frac{1}{2}\rho S d CM_{CG}}} \text{ metres}$$

$I$  is the moment of inertia about the vehicle CG in the pitch or yaw axis, which is constant after burnout.  $\rho$  is air density, varying slowly with altitude. So this formula suggests that this 'wavelength' is a constant distance as there are no airspeed terms.

Though rather screaming assumptions were made in the derivation of this formula, I'm assured that it works over moderate changes of airspeed (Mach number), so that if this distance can be measured, then an average small-angle of attack  $CM_{CG}$  can be calculated.



## Technical papers

---

This wavelength can be recorded on video, or using an onboard flight computer that can measure Normal accelerations as well as Axial accelerations to give distance with time and the number of oscillations over time, such as the new RDAS tiny. Measurements averaged over ten oscillations or so is said to give an accurate result.



## **8: Applicability and accuracy**

Aerodynamics is an inexact science at our present state of knowledge and computational power. Various assumptions have to be made when trying to deal with the motion of billions of air molecules. This means that the aerodynamic coefficients presented earlier are only so exact; a tolerance has to be applied to them.

For example, the drag coefficient is very inexact (perhaps  $\pm 0.1$  in the transonic zone) so sim a trajectory using both ends of this tolerance band to get upper and lower apogees.

The tolerances and applicabilities of the ESDU sheets are:

ESDU 89008:

Freestream Mach numbers of 0 to 5, nose lengths of 1.5 to 7.0 calibres, cylindrical fuselage lengths of 10 to 20 calibres (the paper provides a factor to deal with lengths down to zero), Body-length Reynolds numbers of  $10^5$  to  $10^9$

Tolerances (assuming viscous corrections have been applied):  $\pm 10\%$  on  $C_{N\alpha 0}$ ,  $\pm 5\%$  of vehicle length on 'zero' angle of attack centre of pressure, but note that the effect of centre of pressure movement in the transonic zone wasn't modelled as the data ESDU had to work with was poor in this zone.

ESDU 89014:

Freestream Mach numbers of 0 to 4.5, nose lengths of 0.75 to 6.28 calibres, vehicle lengths of 6 to 22.3 calibres.

Tolerances (assuming viscous corrections have been applied):  $\pm 15\%$  on  $C_N$ ,  $\pm 5\%$  of vehicle length on 'zero' angle of attack centre of pressure, but note that the effect of centre of pressure movement in the transonic zone wasn't modelled as the data ESDU had to work with was poor in this zone.

ESDU 87033:

Freestream Mach numbers of 0 to 5, boat-tail lengths of 0.5 to 1.9 calibres, ratio of boat-tail small diameter over vehicle diameter 0.6 to 0.91, slope of boat-tail 2.5 to 10 degrees, angle of attack 0 to 60 degrees.

Note that for slope of boat-tail angles greater than about 10 degrees, the flow separates (doesn't follow the slope) which alters the lift from that given in this paper. Boat-tails with flow separation just cause drag, and so are to be avoided.

Tolerances:  $\pm 10\%$  on  $C_{Na}$ ,  $\pm 0.02$  on  $C_N$ , unknown tolerance on centre of pressure position due to scatter in the windtunnel data.

ESDU 93034:

The method of this Item is restricted to thin, sharp-edged, uncambered and untwisted wings with straight leading edges, straight unswept trailing edges and streamwise tips.

Tolerances:  $\pm 15\%$  on  $C_{Na0}$ ,  $\pm 5\%$  on  $C_N$

ESDU 90013:

The method of this Item is restricted to thin, sharp-edged, uncambered and untwisted wings with straight leading edges, straight unswept trailing edges and streamwise tips.

Tolerances:  $\pm 15\%$  on  $C_{Na0}$ ,  $\pm 0.05$  on  $\frac{X_{Fins}}{\text{root chord length}}$



ESDU 95022:

The method of this Item is restricted to thin, sharp-edged delta, cropped-delta and rectangular wings without camber or twist.

Tolerances:  $\pm 3\%$  of fin root chord for aerodynamic centre.

ESDU 91007:

The lift-curve slopes and lift coefficients for wing-body combinations derived from the method of this Item are applicable to low angles of attack when viscous cross-flow effects are unimportant.

Tolerances:  $\pm 10\%$  on  $C_{Na0}$  and  $C_N$

ESDU 92024:

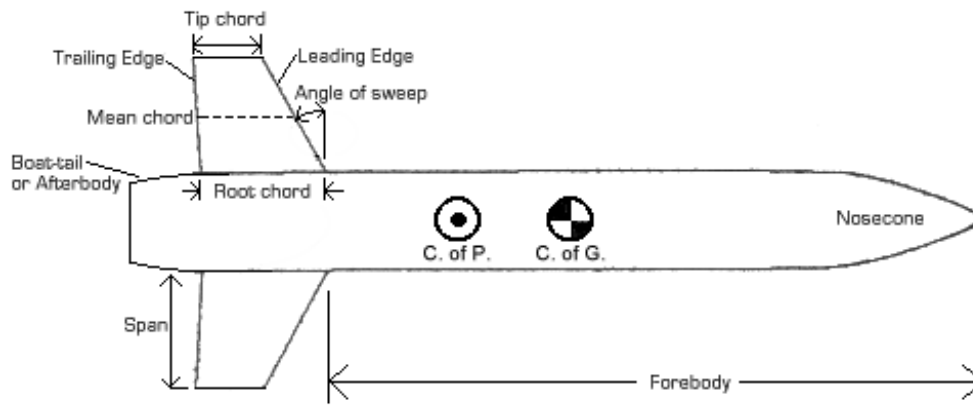
The method of this Item is restricted to thin straight-tapered wings mounted at mid-height on an axisymmetric body. The method is only applicable to low angles of attack where viscous cross-flow effects can be neglected.

Tolerances:  $\pm 0.02$  of vehicle length on aerodynamic centre position.

I'm sure the formulas within the above ESDU sheets can be applied outside of the stated ranges, the data will then just be less accurate.

## Glossary

### Geometric definitions:



(strictly, the forebody is everything upstream of the boat-tail when there are no fins present.)

### Angle of attack: $\alpha$ (or Angle of Incidence)

This is usually referred to as 'alpha', and corresponds to the angle between the incoming airflow direction (usually the **Freestream** direction) and some vehicle or fin datum.

### Aspect ratio AR:

A wing or fin's wingspan divided by its width (or mean chord, see above **geometric definitions** diagram.)

### Bernoulli's principle:

Is just a statement of the Law of Conservation of Energy couched in aerodynamic terms (see

**Dynamic Pressure**) and is expressed in the equation:  $P + \frac{1}{2}\rho V^2 = \text{constant}$ ,

or:  $\Delta P = -\frac{1}{2}\rho \Delta V^2$  where  $P$  is pressure,  $\rho$  is density, and  $V$  is flow velocity.

### Calibres, Calibers:

In rocketry, vehicle dimensions are usually divided by (compared to) the diameter of the thickest part of the fuselage so that rockets of different size can be compared: this diameter is therefore one Calibre.

### Centre of Gravity, centre of mass (CG):

The point within the vehicle that is the centroid of mass, the balance point.

### Centre of Pressure (CP):

The point on the rocket's surface where the average of all the aerodynamic pressure forces from the nose, body, and fins act. This must be behind the Centre of Gravity (CG) by at least one **Calibre** for stability.

### Drag (equation):

Drag, or 'air resistance', is the retarding force experienced by bodies travelling through a fluid (gas or liquid).

The equation used to calculate drag is simply the *drag coefficient*,  $C_d$ , times **dynamic pressure**, times some reference area 'S', i.e:  $(\rho = \text{atmospheric density.})$

For the rocket vehicle, this reference area 'S' is the maximum cross-sectional area of the fuselage (ignoring the fins or small, local structures), whereas for aircraft, it's the total wing area.

**Dynamic pressure: (q)**

All aerodynamic forces scale directly with the kinetic energy term:  $\frac{1}{2}\rho V^2$

$\rho$  being volume-specific mass or air density, and  $V$  = flow velocity.

This kinetic energy term is called Dynamic Pressure (q), to distinguish it from its Potential energy counterpart of static pressure (P).

**Flowfield:**

The flowfield, as the name suggests, comprises the airflow and its **properties** within a general volume of interest.

If the flow properties at all points in the flow don't vary with time, then the flowfield is said to be steady.

**Forebody:**

The nosecone and forward fuselage.

**Freestream (flowfield):  $\infty$**

The undisturbed airflow at a large ('infinite') upstream distance ahead of the **vehicle**, i.e. not **local**. For example, freestream **Mach number** is Mach number for the whole vehicle as we'd usually understand it, and not the **local** Mach number around the nosecone or fins.

Freestream **properties** have the subscript  $\infty$ , and are those of the atmosphere.

**HPR:** 'High-powered rocket' a model/amateur rocketry designation denoting a rocket powered by H to O class engines.

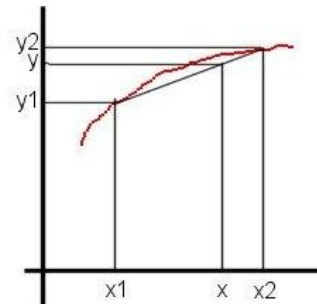
**Linear interpolation:**

To get a value that is inbetween a pair of values in a table you interpolate between the values. Linear interpolation joins the pair of values with a straight line.

For example, suppose you want the value 'y' corresponding to 'x' in this graph. 'x' is  $\frac{3}{4}$  closer to  $x_2$  than  $x_1$ , so 'y' will be  $\frac{3}{4}$  closer to  $y_2$  than  $y_1$ .

The formula is:  $y' = m'x' + C$

where  $m = \frac{y_2 - y_1}{x_2 - x_1}$  and  $C = y_1 - m x_1$



**Local (flowfield):**

The airflow (**properties**) in the immediate vicinity of the vehicle i.e. not **Freestream**.

**Mach number:**

The vehicle's airspeed  $V$  (or the **local** airspeed around a nose or fin) compared to the speed of sound 'a':

$$M = \frac{V}{a}$$

**Pitching moment coefficient:  $C_m$**

The lift force of the fins and nosecone (and boattail) causes a torque that rotates the vehicle. In stability analyses we usually require to calculate the torque about a fictitious pivot at the nosecone tip.

The coefficient is:  $C_m = \frac{T}{\frac{1}{2}\rho V^2 d}$  where  $T$  is the torque and  $d$  is fuselage (max) diameter.

**Planform area:**

The area of a two-dimensional drawing of the vehicle, showing it side-on, or the surface area of one side of a fin.



**Pressure coefficient:  $C_p$**

Is the **local** pressure (P) compared to some reference pressure (**Freestream**) and divided by

the local **Dynamic pressure**:  $C_p = \frac{P - P_\infty}{\frac{1}{2}\rho V^2}$  (see **Bernoulli's principle**.)

**Properties:**

Measurable or derivable quantities comprising the usual thermodynamic properties (pressure P, density  $\rho$ , temperature T, etc) plus extra flow properties such as flow direction and flow velocity V.

**Reference area: (S)**

See Drag (equation)

**Skin:**

The outer covering or surface of the vehicle.

**Subsonic:**

Vehicle airspeed is below Mach 1 (see **Mach number**).

**Supersonic:**

Vehicle airspeed is above Mach 1 (see **Mach number**).

**Stagnation point:**

At zero angle of attack, the air encountering the very tip of the nose stops dead (becomes stagnant), and gives up its kinetic energy by increasing its pressure. This is because real nosetips have some radius of curvature, however slight. This higher pressure is known as the stagnation pressure, and can be captured in a tube sticking out from the nose called a Pitot tube.

At angle of attack, the stagnation zone moves a little way off of the nosetip down the nosecone.

**Taper ratio:**

The ratio of fin tip chord divided by fin root chord (see above diagram 'geometric definitions').

**Transonic:**

Above a **freestream Mach number** of about 0.7, certain parts of the **local** flow around the nose and fins will hit a local Mach of above 1.0, **supersonic**.

Similarly, up to a freestream Mach number of about 1.4, certain parts of the local flow around the nose and boat-tail are still **subsonic**.

The transonic zone is this freestream Mach number region where there is a mix of subsonic and supersonic flow. This mixture makes predicting the aerodynamics of the zone difficult and inexact.

**Vehicle: (the)**

A stationary object immersed in a moving airflow, or an object moving through stationary air. (Aerodynamically, these two situations are identical in every respect.)

Here, the vehicle is a rocket-vehicle.

**Viscosity:**

Viscosity, just as in car engine oil grades, is basically the 'syruiness' of the fluid.

3-in-1 oil having low viscosity, and thick tar having high viscosity.

Viscosity is technically defined as resistance to shearing (rate) of fluid.



## References

1. 'The Theoretical Prediction of the Centre of Pressure', James S. Barrowman and Judith A. Barrowman, NARAM-8 R&D Project, 1966  
[http://www.apogeerockets.com/education/downloads/barrowman\\_report.pdf](http://www.apogeerockets.com/education/downloads/barrowman_report.pdf)
2. 'The practical calculation of the aerodynamic characteristics of slender finned vehicles' J. Barrowman, Master's thesis.  
[http://ntrs.nasa.gov/archive/nasa/casi.ntrs.nasa.gov/20010047838\\_2001074887.pdf](http://ntrs.nasa.gov/archive/nasa/casi.ntrs.nasa.gov/20010047838_2001074887.pdf)
3. 'Lift and center of pressure of wing-body-tail combinations at subsonic, transonic and supersonic speeds' Pitts, W.C., Nielsen, J.N., Kaattari, G.E. NACA Report 1307, 1957, Downloadable at <http://naca.central.cranfield.ac.uk/report.php?NID=6866>
4. Engineering Sciences Data Units (ESDU sheets) [www.esdu.com](http://www.esdu.com)
5. 'Calculation of the centre-of-pressure of a rocket', Rocket Services technical report, J. Pitfield, 1988
6. Mathematical theory of rocket flight, Rosser, Newton, Gross, McGraw-Hill Inc 1947 (now back in reprint from Amazon)
7. 'Fundamentals of dynamic stability' by Gordon K. Mandell, National Association of Rocketry NAR Tech. Report TR-201, Fuselage cross sectional area is denoted here as (A) instead of the original  $A_r$  as this can be confused with Aspect Ratio, Note that this analysis is described in a series of articles in Apogee newsletters 195-198  
[http://www.apogeerockets.com/education/newsletter\\_archive.asp](http://www.apogeerockets.com/education/newsletter_archive.asp)
8. 'Wind caused instability', Bob Dahlquist, High power rocketry magazine March 1988
9. 'Development of an Open Source model rocket simulation software' Sampo Niskanen, Helsinki University of Technology, Faculty of Information and Natural Sciences
10. 'A design procedure for maximising altitude performance' Edward D. LaBudde, Submitted at NARAM 1999
11. 'The aerodynamics of guided weapons' Cranfield University course, 1970
12. 'Understanding aerodynamics – arguing from the real physics', Doug McLean, Wiley, 2014